THESIS

DISPERSION IN BI-MODAL OIL SHALES

Submitted by

Mark A. Bryant

College of Civil Engineering

In partial fulfillment of the requirements

for the Degree of Master of Science

College of Engineering

Colorado State University

Fort Collins, Colorado

Spring, 1982

COLORADO STATE UNIVERSITY

Spring 19 82

WE HEREBY RECOMMEND THAT THE THESIS PREPARED UNDER OUR SUPERVISION

BY Mark A. Bryant

ENTITLED Dispersion in Bi-Modal Oil Shales

BE ACCEPTED AS FULFILLING IN PART REQUIREMENTS FOR THE DEGREE OF

Master of Science

Committee on Graduate Work

Daniel K. Sunada

Robert C. Ward

David B. McWhorter

Adviser

ABSTRACT OF THESIS

DISPERSION IN BI-MODAL OIL SHALES

A series of leaching column experiments were conducted using 3 different grain sizes of spent oil shale from the Paraho retorting process. Electrical conductivity breakthrough data produced at 3 different seepage velocity rates were analyzed with the help of a least squares curve fitting computer model, CFITIM, developed by Van Genuchten (1981). Emphasis was placed on the identification of transport mechanisms which could explain the observed asymetry of the breakthrough curves.

Comparison of the column breakthrough curves to a analytical dispersion model which took into account a micro pore diffusion transfer mechanism, produced poor correlation. When a linear sorption transfer mechanism was coupled with a micro pore diffusion transfer mechanism in the analytical model a much better match of the breakthrough data was obtained.

The analytical model may prove useful in the development of a standard leaching column test procedure, however, it is suspected that the model parameters have little physical significance and therefore can only be used in fitting the breakthrough curves.

Mark A. Bryant
Civil Engineering Department
Colorado State University
Fort Collins, Colorado 80523
Spring, 1982

ACKNOWLEDGMENTS

The author wishes to express his gratitude to his major professor, Dr. David B. McWhorter, for the outstanding guidance and advice he gave throughout this study.

The author would also like to thank committee members, Dr. Daniel K. Sunada and Dr. Robert R. Ward, for their discussions and helpful comments on the concepts involved in this study.

Appreciation is also extended to Mr. John Brookman for his valuable help in conducting the laboratory research and in preparing the diagrams and figures used in this thesis. Special recognition must be given to Mrs. Jacquelyn Roberts for her patience and diligence in the typing and preparation of this thesis.

TABLE OF CONTENTS

TABLE OF CONTENTS (continued)

LIST OF FIGURES

LIST OF TABLES

LIST OF SYMBOLS

Symbol		Units
A	Area of column	L^2
a	Dimensionless constant	
b	Dimensionless constant	
C	Concentration of tracer	M/L^3
C_{im}	Tracer concentration in the immobile fluid region	M/L^3
C_m	Tracer concentration in the mobile fluid region	M/L^3
C_o	Initial tracer concentration	M/L^3
C_1	Normalized concentration of tracer in the mobile fluid region	
C_2	Normalized concentration of tracer in the immobile fluid region	
D	Hydrodynamic disperson coefficient	L^2/T
D_t	Fluid residence time	T
f	Fraction of adsorption sites in contact with the mobile fluid	
I_o	Modified Bessel function	
I_1	Modified Bessel function	
k	Adsorption rate coefficient	L^3/M
L	Length of column	L
P	Peclet number	
Q	Average column flow rate	L^3/T
R	Retardation factor	

Symbol		Units
S	Tracer concentration adsorbed	M/M
T	Pore volume	
t	Time	T
V	Mean pore velocity	L/T
V_m	Mean pore velocity in the mobile fluid region	L/T
V_s	Seepage velocity, the mean pore velocity in the macro pore regions	L/T
x	Space coordinate	L
Z	Dimensionless distance	
α	Diffusional rate coefficient	T^{-1}
β	Dimensionless variable	
θ	Volumetric water content	L^3/L^3
θ_{im}	Portion of volumetric water content making up the immobile fluid region	L^3/L^3
θ_m	Portion of volumetric water content making up the mobile fluid region	L^3/L^3
ϕ_t	Total volumetric porosity	L^3/L^3
ϕ_{macro}	Macro porosity; the portion of volumetric porosity made up of macro pore space	L^3/L^3
ϕ_{micro}	Micro porosity; the portion of volumetric porosity made up of interconnected micro pore space	L^3/L^3
ϕ^{ω}_{micro}	Volume of interconnected micro pore space per unit dry weight of solids	L^3/M
ξ	Dimensionless constant	
ρ	Bulk density	M/L^3

Symbol		Units
ρ_p	Apparent particle density; the dry weight of solids per unit volume of solids	M/L^3
τ	Integration variable	
ω	Dimensionless rate constant	

CHAPTER I

INTRODUCTION

A. Background

Oil shale development in the western United States is receiving an increasing amount of attention as we look for domestic sources of energy to replace uncertain foreign supplies. While oil shales are found in many parts of the United States (see Figure 1), the richest and most extensive deposits are found in the Green River Formation in Colorado, Utah, and Wyoming. The total identified shale oil resource in the United States is estimated by the USGS to be over 270 billion tonnes (two trillion barrels) (USEPA Draft Report, 1979). Of this amount, over 90 percent, or an estimated 251 billion tonnes (1,842 billion barrels), is found in the Green River Formation.

The oil shale resource in the Green River Formation is distributed in the Piceance Creek basin in Colorado, the Uinta basin in Utah, and the Green River and Washakie basins in Wyoming (see Figure 2). These deposits contain about 80 billion tonnes (590 billion barrels) of shale oil considered by the USGS to be 'potentially recoverable' (oil shales at least 10 feet thick containing 25 gallons/ton or more of oil). This is equivalent to more than an 85 year oil supply at the 1978 U.S. consumption rate. More than 80 percent of these commercially attractive oil shale resources are in Colorado's Piceance basin.

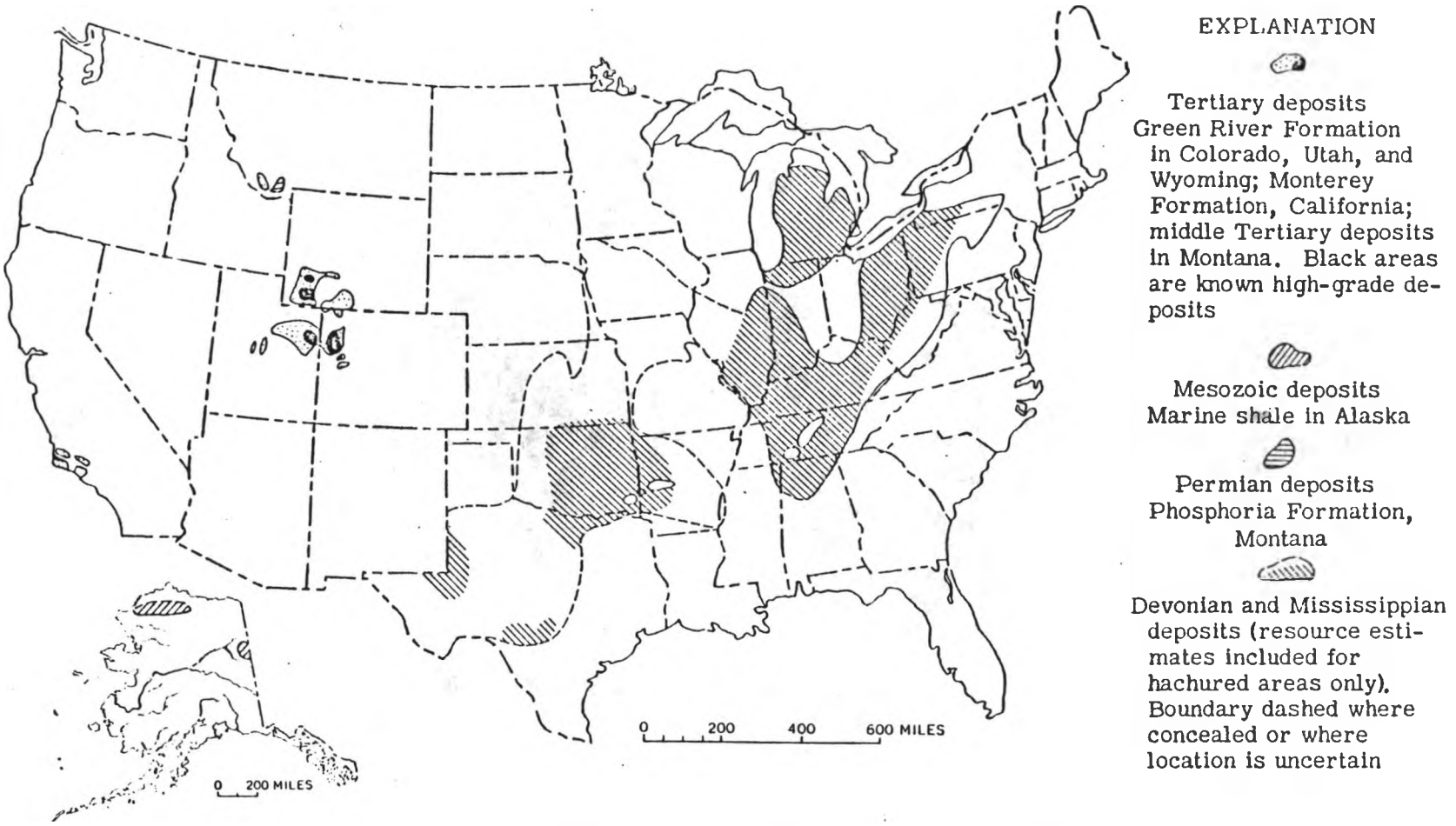

FIGURE 1. PRINCIPAL REPORTED OIL SHALE DEPOSITS OF THE UNITED STATES. (From Geological Survey Circular 523, 1965.)

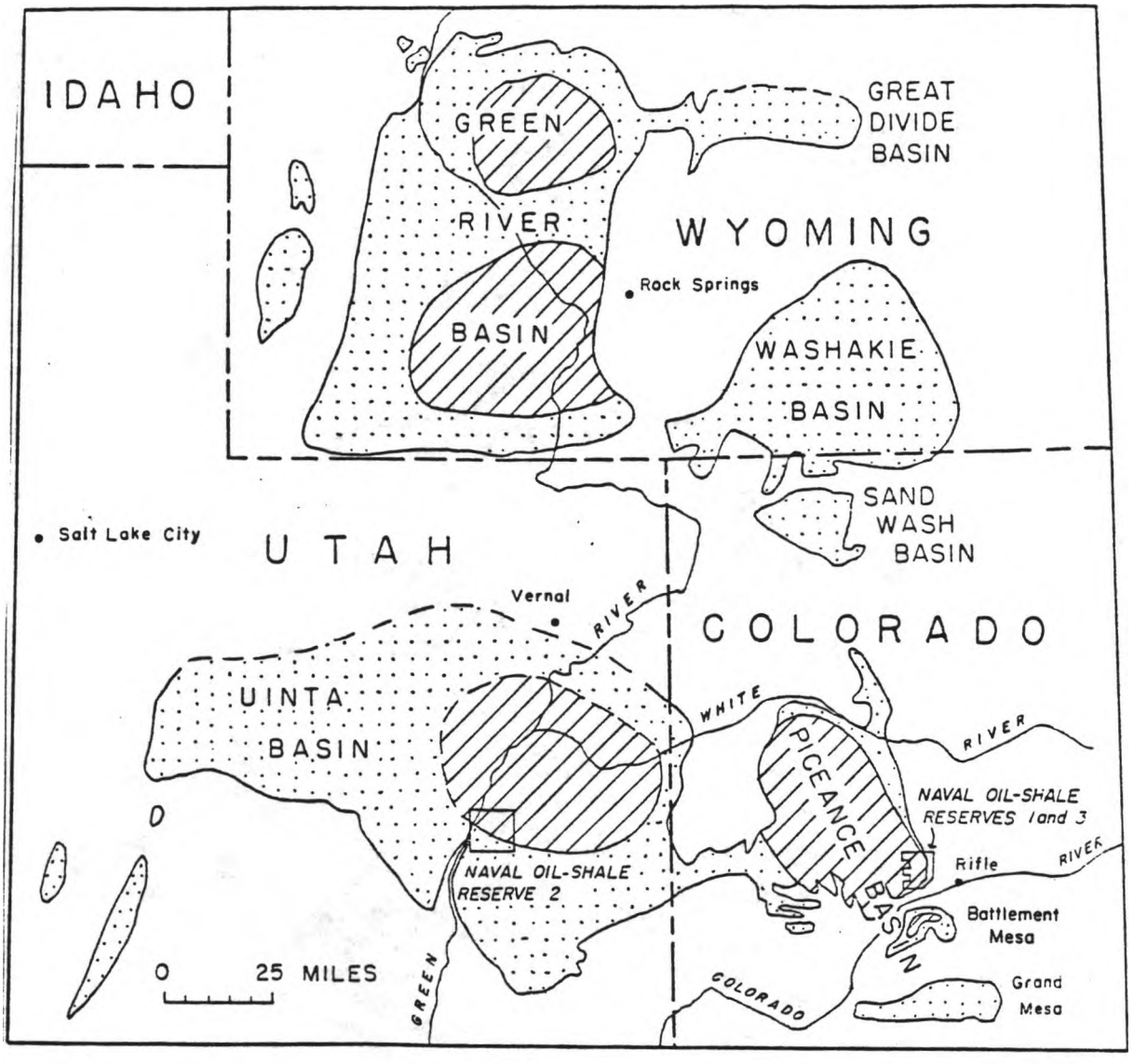

EXPLANATION

Area underlain by the Green River Formation in which the oil shale is unappraised or low grade

Area underlain by oil shale more than 10 feet thick, which yields 25 gallons or more oil per ton of shale

FIGURE 2. DISTRIBUTION OF OIL SHALE IN THE GREEN RIVER FORMATION, COLORADO, UTAH, AND WYOMING. (From Geological Survey Circular 523, 1965.)

The Green River Formation was formed from the deposition of silt, sand, and plant and animal debris on the beds of prehistoric lakes; Lake Gosiute in Wyoming and Lake Uinta in Colorado and Utah. With the passage of time, geologic and climatic changes caused the lakes to dry and the lake deposits to form layers of marlstone, sandstone, siltstone, limestone, and tuff. The organic materials were converted to a solid hydrocarbon called kerogen; oil shale is actually a marlstone that is rich in kerogen.

In the Piceance basin (see Figure 3), the Green River Formation is bounded on top by the Uinta Formation and below by the Wasatch Formation. The Uinta formation varies in depth from 0 to about 1,000 feet, and is made up mostly of sandstone and siltstone with some low grade oil shale. The Green River Formation ranges in thickness from a few hundred feet to about 7,000 feet, and is made up, in descending order, of the Parachute Creek member, the Garden Gulch member, the Douglas Creek member, and the Anvil Points member (Duncan and Swanson, 1965). The Parachute Creek member contains the most commercially attractive beds of oil shale, the most noteworthy of which is known as the Mahogany zone. The Mahogany zone is the richest layer of oil shale, ranging in thickness from 100 to 200 feet. It outcrops in many areas of the basin, while at other locations it is covered by over 1,000 feet of overburden. Generally, the thickest and richest oil shale layers occur in the central areas of the individual basins, with the Green River and Washakie basins having thinner and leaner oil shale beds than the Piceance and Uinta basins.

In order to extract the oil from the shale, the shale is heated to temperatures of about 900° F in a pyrolisis process, which causes the

Geologic Unit	Unit Subdivisions		Lithologic Description	Hydrologic Unit	Water-Yielding Properties
Valley Alluvium 0' - 140'	—		Sand, Gravel, Clay	Alluvial Aquifer	Limited in areal extent and thickness. 1500 gpm maximum.
Uinta Formation 0' - 1250'	—		Mainly sandstone and siltstone with minor amounts of low-grade oil shale and barren marlstone.	Upper Aquifer	Well yields about 100 gpm. TDS from 250 to 1800 ppm.
Green River Formation	Parachute Creek Member 500' - 1600'	Upper Part of Parachute Creek Member			
		Mahogany Zone	Moderate-to-high-grade oil shale	Aquitard	Low permeability. Limited percolation through vertical fracture is important in regional ground water flow.
		Leached Zone	Low-to high-grade oil shale.	Lower Aquifer	Best developed in north central part of basin. Confined aquifer. Wells may yield 1000 gpm. About 2000 ppm TDS near edges to 45,000 TDS near center.
		High-Resistivity or Saline Zone	Saline minerals and moderate-to high-grade oil shale.	Aquitard	Relatively impermeable.
	Garden Gulch member 0' - 900'		Mainly clayey shale and low - to moderate-grade oil shale.	Aquitard	Relatively impermeable
	Douglas Creek member 0' - 800'		Mainly sandstone with minor amounts of limestone.	Minor Aquifer	Relatively impermeable About 350 gpm well yields. TDS from 3000 to 12,000 ppm.
	Anvil Points member 0' - 1670'		Shale, sandstone, marlstone.	Minor Aquifer	Relatively impermeable
Wasatch Formation				Aquitard	Relatively impermeable

FIGURE 3. DETAILED STRATIGRAPHY OF GREEN RIVER FORMATION. (From USEPA "Pollution Control Guidance for Oil Shale Development", revised draft report, July 1979.)

kerogen to vaporize and separate from the shale. These vapors are then condensed to form liquid shale oil and product gases. A number of retorting processes are under study at the present time in various stages of development. These can be classified as either surface retorting processes or in situ retorting processes.

Surface retorting processes involve a number of general steps including:

Mining - the oil shale is removed by either underground or surface mining.

Crushing, transportation and storage - the oil shale is removed from the mine, prepared for retorting, and stockpiled until needed for feed in the retort.

Retorting - the raw shale is heated and the shale oil and product gases removed for further refining and use.

Cooling and disposal of spent shale - the waste shale from the retort is stockpiled, cooled, and ultimately disposed.

Some of the surface retorting processes being considered for commercial operation at this time include the TOSCO II process, the Paraho process, the Union Oil B and SGR processes, the Superior process, and the Lurgi-Ruhrgas process. Among other process configuration differences, these differ in the size of shale fragments used in the retort, the method used in heating the shale, and the source of fuel used to supply the heat for retorting. The TOSCO II and Lurgi-Ruhrgas processes require a finely crushed feed stock, which produces a fine powder like spent shale. The other processes use larger particle sizes which produce spent shale fragments up to 8.9 cm (3 1/2 inches) in diameter. Spent shale will contain residual carbon which can be used as a fuel

source. If this residual carbon is utilized the spent shale will change from a dark gray or black to a lighter color. The Union Oil SGR, Superior, and Lurgi-Ruhrgas processes utilize this residual carbon, while the TOSCO II and Union Oil B processes do not. The Paraho process can be operated in either a direct-heated mode, which utilizes the residual carbon, or an indirect-heated mode, which does not.

In situ processes involve the retorting of shales in place underground. The shale is fractured to establish adequate permeability, then heated to remove the oil and product gases. It has the advantage of eliminating the mining, transportation, storage, and disposal requirements of surface retorting techniques; but there are problems in achieving adequate fracturing in the shale prior to retorting, and also in adequately controlling the retort process. Because of these problems, a modified in situ process is usually considered instead of a true in situ process. In a modified in situ process, approximately 20 percent of the raw oil shale is removed by mining in order to provide void space for fracturing. The remaining shale is then hydraulically or explosively fractured and then retorted. The shale oil produced flows by gravity through the rubblized shale to a sump at the bottom of the retort zone, where it is pumped to the surface. A modified in situ process would likely be coupled with a surface retort to process the oil shale removed for void space.

Although there is much interest in both the true and modified in situ retorting processes, the modified in situ retorting processes of Occidental Petroleum Company and Rio Blanco Oil Shale Company are the only ones which have been developed to the degree of the surface retorting processes.

Regardless of the retorting process used, the quantities of raw and spent shales involved in a commercial size shale oil industry will be great. The size of a mature shale oil industry range from a Presidential goal of 400,000 bbl/day, set in 1979, to industry estimates of one to two million bbl/day by the year 2000. A single commercial-size operation producing 50,000 bbl/day will require more than 77,000 tons per day of raw oil shale (assuming 90 percent yield of 30 gal/ton oil shale). After the oil is removed, approximately 65,000 tons of spent shale (85 percent by weight of the raw mined oil shale), will be left for disposal. At a maximum compaction density of 100 lbs/ft ^{3} this will amount to approximately 1.3 million cubic feet (144,400 cubic yards) per day. In the course of a year, this amounts to enough spent shale to cover a one square mile area to a depth of 17 feet. When these estimated quantities are multiplied by the life of the retort and by the number of retorts needed to total the expected industry shale oil production, it can be seen that the size of the mining and waste disposal aspects of a mature oil shale industry will be on a scale never before seen in this area of the country.

Disposal of these quantities of spent shales presents a major problem. In situ processes, of course, leave the spent shale in the ground. Surface retorted shale, however, must be stored and a location found for final disposal. One logical disposal site to consider would be back in the mine from where the shale originally came. The logistics and expense of transporting and disposing the spent shale, while conducting an active mining operation, however, make this method unlikely. It should also be noted that spent shale occupies a larger volume than the

original in-place shale. Because of this, total disposal in an underground mine is not possible. The most likely disposal method to be used is above ground, either filling existing canyons or compacting and contouring the spent shale on relatively flat terrain.

There is much concern for the impact these raw and spent oil shale storage and disposal piles will have on area water quality. Waters which may migrate through these piles will pick up various contaminants which may find their way into the surface and ground waters. Knowledge of the chemical species involved, their concentrations and rates of release must be known in order to predict and assess this impact. To do this, test procedures are needed which will accurately predict the leachate quality.

A variety of tests could be used for this purpose, including:

A. total digestion of the material in question to determine the total quantities of chemicals present,

B. agitation tests such as the RCRA extraction test or the ASTM Water Shake extraction test to determine the total quantities of soluable materials present,

C. column leaching tests to determine chemical concentrations and rates of release under laboratory conditions,

D. lysimeter leaching tests to determine chemical concentrations and rates of release under field conditions.

Total digestion and agitation tests can give useful information on the chemicals present and the total quantities involved; however, they do not give information on the rates of release and concentrations to be expected. Column leaching and lysimeter leaching tests are more desirable from this standpoint. Although lysimeter studies would give

results which more nearly reflect the actual field conditions, the time, expense, and lack of controls associated with field testing make it undesirable for use as a standard predictive test procedure. Laboratory leaching column tests can give relatively fast and inexpensive results, but it is not known if these results can be extrapolated to reflect field conditions. The first step towards resolving this question is to acquire a basic understanding of the chemical transfer mechanisms involved.

Leaching column tests can be conducted a number of different ways. One commonly used method is to establish steady flow through a packed column then switch influent sources from water to that of water containing a known concentration of a chemical. this chemical is known as a tracer. By monitoring the tracer concentration in the column outflow with time, a tracer breakthrough curve is produced which describes the transport of that tracer through the column medium. If the transport mechanisms are understood, system parameters can then be calculated which define the interaction of the tracer with the medium. It is then assumed that these parameters can be used to predict this tracers' transport in the full-scale situations of interest. It is important to note that the tracer breakthrough curve is dependent on the particular chemical being monitored. If a different chemical is used as the tracer, a different tracer breakthrough curve will be produced.

When considering the migration of water through oil shale stock piles, various chemical species will be added to the water from the oil shale medium. A leaching column test which more closely approximates this situation is one which uses a chemical species contributed by the oil shale medium as the tracer. One method of doing this (which is the

method used in this investigaton), is to saturate a packed column with water initially containing no concentration of the chemical to be monitored. Time is then allowed for the tracer to leach from the medium to the water and for chemical equilibrium to be reached. At a particular time steady flow of tracer free water is established through the column. Monitoring the chosen tracer concentration with time in the outflow will produce a tracer breakthrough curve.

B. Purpose and Scope

The objective of this investigation is to study chemical transport mechanisms in saturated leaching column tests using a spent oil shale media. Particular emphasis is placed on how media particle size and porosity effects the transport mechanisms. It is hoped that an improved knowledge of the transport process can be gained that will lead to the development of a standardized leaching column test procedure.

It is not proposed to determine the chemical quality of leachates from oil shales, or is there any intention to extrapolate the results of these laboratory tests to field situations. This study is part of a larger program investigating these and other aspects of the hydrologic properties of oil shales. The results of this study should be useful in subsequent investigations of these hydrologic properties.

For this study a series of nine leaching column tests were conducted using three different particle sizes of retorted oil shales from the indirectly-heated Paraho process. Bulk densities and fluid residence times were controlled, while seepage velocities were varied. Distilled water was used to displace water in the columns, which had come to chemical equilibrium with the media. By monitoring the

electrical conductivity of the effluent as an indication of the total salt concentration, a tracer breakthrough curve could be calculated. In addition, a leaching test using a pulse flow of NaCl solution as a tracer was conducted using one of the leached spent shale columns.

The results were analyzed using models which incorporated different transfer mechanisms in order to determine the adequacy of these mechanisms in explaining the results.

CHAPTER II

LITERATURE REVIEW

The transport of a chemical species (tracer) through a non-reactive homogeneous porous media is generally modeled by the advection-dispersion equation, (Lapidus and Amundson, 1952):

$$D \frac{\partial^2 C}{\partial x^2} - V \frac{\partial C}{\partial x} = \frac{\partial C}{\partial t} \qquad (1)$$

where D = hydrodynamic dispersion coefficient (L^2/T)

C = tracer concentration (M/L^3)

V = mean pore velocity of the solution (L/T)

t = time (T)

x = space coordinate (L)

A solution to Equation (1) subject to the initial and boundary conditions

$C = 0$ at $x > 0$, $t = 0$

$C = C_o$ at $x = 0$, $t > 0$

$C = 0$ at $x \rightarrow \infty$, $t \geq 0$

is (Nielsen and Biggar, 1962):

$$\frac{C}{C_o} = 0.5 \left[\operatorname{erfc} \left| \frac{x-Vt}{\sqrt{4Dt}} \right| + \exp \frac{Vx}{D} \operatorname{erfc} \left| \frac{x+Vt}{\sqrt{4Dt}} \right| \right] \qquad (2)$$

The dispersion coefficient, D, is the system parameter used to describe the tracer transport process. In this simple situation, D takes into account the mixing of the tracer due to molecular diffusion

and mechanical mixing as it passes through the media. The diffusion mechanism causes mixing by transporting the tracer from areas of high concentration to areas of low concentration. The mechanical mixing is caused by variations in pore velocities. If there were no mixing, (D=0), piston displacement of the original fluid by the tracer fluid would be expected (see Figure 4). However, as long as D is some finite value greater than zero, Equation (2) predicts a symmetrical, sigmoidal breakthrough curve about the point $C/C_o = 0.5$ at 1 pore volume, (see Figure 4).

In leaching column tests conducted on raw oil shales (McWhorter, 1980), highly asymmetrical breakthrough curves were noticed. Since this asymmetry cannot be explained by Equation (2), other transport mechanisms affecting the breakthrough must be taken into account. One possible cause of this tailing effect of the breakthrough curve is the pore space contained in individual media fragments. The oil shale fragments will exhibit a primary porosity made up of the pore space within each individual fragment, while the aggregated media will also exhibit a secondary porosity made up of the pore space between the fragments. Since the secondary (macro) pore size is orders of magnitude larger than the primary (micro) pore size, the bulk flow of leaching waters through the media will occur in the macro pore space. Fluids contained in the micro pore space, therefore, will not be physically displaced by the flowing fluid. Instead, diffusion is expected to control the transfer of the tracer into (or out of) the micro pore space. In conducting leaching tests with a media exhibiting this bi-modal property, one would expect the breakthrough curve to rise rapidly as the tracer solution displaces and mixes with the fluid in the macro pore space, then tail

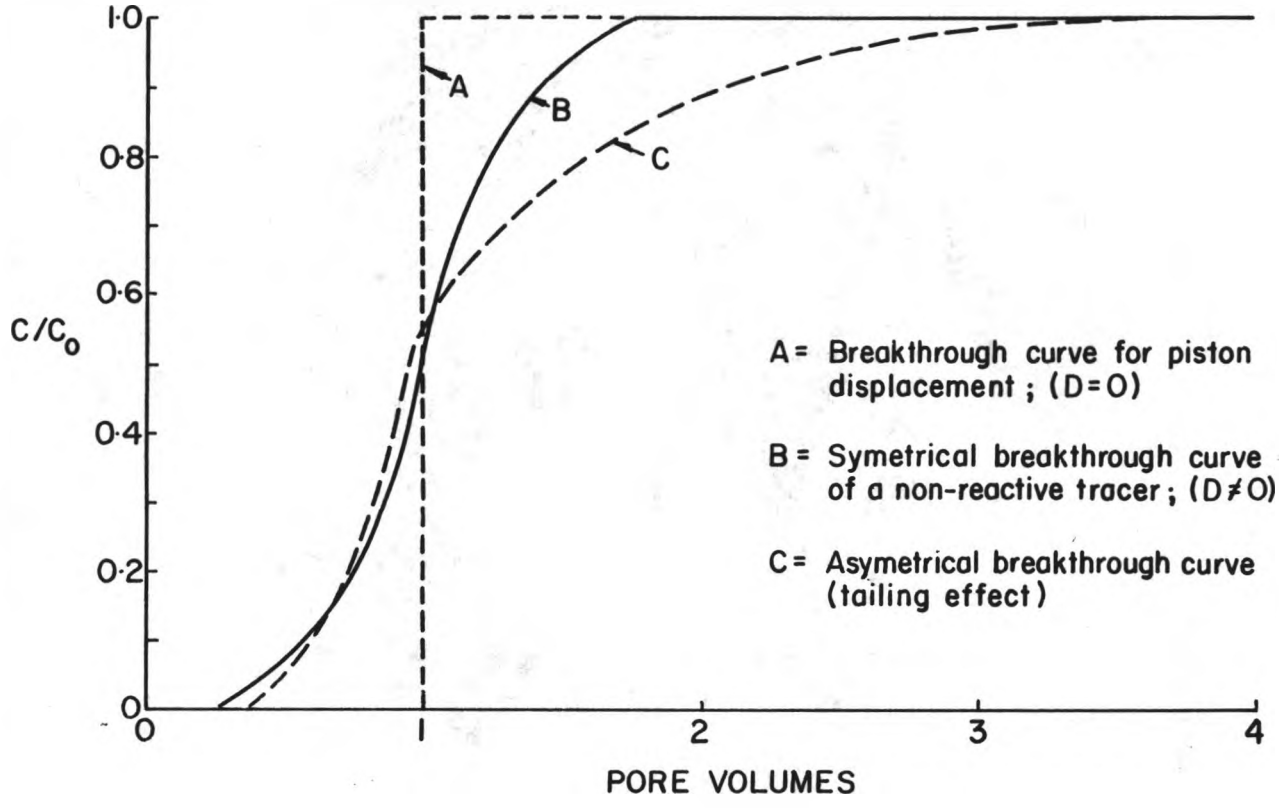

Figure 4. THEORETICAL NORMALIZED BREAKTHROUGH CURVES FOR A NON-REACTIVE TRACER

off slowly as diffusion of the tracer into the micro pore space controls the tracer transfer, (see Figure 4). This tailing effect would be expected to be particularly pronounced in a spent oil shale medium as there would be enhanced micro porosity caused by the vaporization and removal of the kerogen during retorting.

The terminology used in the literature which is analogous to the term micro porosity used in this study includes dead end pores, stagnant pockets, capacitance, and immobile water regions. All of these terms make a distinction between the portion of the total pore volume which contributes to bulk flow, and that portion which does not.

It should be noted that although a bi-modal porosity is one possible explanation of a tailing effect on breakthrough curves, other mechanisms could also cause or contribute to this effect. These include:

A. chemical reaction processes,

B. adsorption-desorption processes.

Any or all of these mechanisms could be taking place and interacting with each other in some complicated manner.

In studies of dispersion in bi-modal media, it has been found that Equation (2), or similar solutions, does not adequately predict the breakthrough curve. Biggar and Nielson (1962) investigated micro pore diffusion effects by conducting leaching column tests on three sizes of Aiken clay loam aggregates. Using two tracers having unequal diffusion coefficients, chloride and tritium, the contribution of diffusion to the tracer transport process could be seen by observing the difference in breakthrough curves. They found that with increasing aggregate size, the tracer appeared earlier and required a larger number of pore volumes

to reach $C/C_o = 1.0$. Also, the breakthrough curves were retarded with decreasing aggregate size, and the tracer having the greater diffusion coefficient, tritium, produced a breakthrough curve which was retarded compared to the chloride breakthrough curve. They attributed these characteristics to differences in velocity distribution and diffusion into the micro pores. With increasing aggregrate size, they theorized that there would be a larger size difference between the micro and macro pores, thereby increasing the proportion of the total flux which goes through the macro pores. This would decrease mixing of the tracer in the column, which would cause it to show up in the effluent sooner. Biggar and Nielsen concluded that the breakthrough curve for the tracer with the greater diffusion coefficient was retarded because faster diffusion into the micro pore space promoted a more rapid mixing of the tracer which decreased the initial tracer concentration. This more rapid mixing would be expected to cause the tracer to reach $C/C_o = 1.0$ before that of the slower diffusing tracer.

Although Biggar and Nielson recognized the possible contribution of micro pore diffusion to the shape of the breakthrough curve, the formulation of dispersion models, which include this transfer mechanism was left to other investigators who have formulated equations to predict breakthrough curves for a media containing dead-end pore volume. Among these are Turner (1958), Goodknight et al., (1960), Philip (1967), Grisak and Pickens (1980), Coats and Smith (1964), Brigham (1974), and Baker (1977). In the formulation proposed by Coats and Smith, equation (1) is modified to include a source/sink term to account for diffusion into (or out of) the immobile water areas (micro pore space). The modified transfer equation (after Van Genuchten and Wierenga, 1976) can be

written as:

$$\theta_m D \frac{\partial C_m}{\partial x^2} - \theta_m V_m \frac{\partial C_m}{\partial x} = \theta_m \frac{\partial C_m}{\partial t} + \theta_{im} \frac{\partial C_{im}}{\partial t} \quad (3)$$

and

$$\theta_{im} \frac{\partial C_{im}}{\partial t} = \alpha(C_m - C_{im}) \quad (4)$$

where θ = volumetric water content of the media (L^3/L^3)

θ_m = portion of the volumetric water content made up of mobile fluid (L^3/L^3

θ_{im} = portion of the volumetric water content made up of immobile fluid (L^3/L^3)

C_m = tracer concentration in the mobile water regions (M/L^3)

C_{im} = tracer concentration in the immobile water regions (M/L^3)

V_m = mean pore velocity of the mobile water regions (L/T)

α = diffusional rate coefficient (T^{-1})

This formulation assumes a first order transfer rate from the immobile water regions to the mobile water regions which depends on the concentration difference between these two regions.

Van Genuchten and Wierenga (1976) further modified the advection-dispersion equations to include the effects of chemical adsorption. By assuming a linear isotherm of the form:

$$S = k C \quad (5)$$

where S = the concentration of tracer adsorbed (M/M)

k = adsorption rate constant (L^3/M)

and by assuming the adsorption sites are split into two fractions, those located in contact with the moving liquid (f) and those located in the immobile liquid regions, (1-f); they obtained:

$$\theta_m D \frac{\partial^2 C_m}{\partial x^2} - \theta_m V_m \frac{\partial C_m}{\partial x} = (\theta_m + \rho f k) \frac{\partial C_m}{\partial t} + \left[\theta_{im} + (1-f)\ \rho\ k\right] \frac{\partial C_{im}}{\partial t} \quad (6)$$

and

$$[\theta_{im} + (1-f)\rho k] \frac{\partial C_{im}}{\partial t} = \alpha(C_m - C_{im}) \quad (7)$$

where ρ = bulk density of media (M/L^3)

Notice that if there is no sorption, k = 0, and Equations (6) and (7) reduce to Equations (3) and (4).

By introducing dimensionless variables, Equations (6) and (7) can be reduced to:

$$\frac{1}{P} \frac{\partial C_1}{\partial Z^2} - \frac{\partial C_1}{\partial Z} = \beta\ R \frac{\partial C_1}{\partial T} + (1-\beta)\ R \frac{\partial C_2}{2T} \quad (8)$$

and

$$(1-\beta)\ R \frac{\partial C_2}{\partial T} = \omega\ (C_1 - C_2) \quad (9)$$

where P = Peclet number $= \frac{V_m L}{D}$; (L = length of column)

$\beta = \frac{\theta_m + f\rho k}{\theta + \rho k}$

R = Retardation factor $= 1 + \frac{\rho k}{\theta}$

T = Pore volumes $= \frac{Vt}{L}$; $V = V_m \frac{\theta_m}{\theta}$

$C_1 = \frac{C_m}{C_o}$

$C_2 = \frac{C_{im}}{C_o}$

$\omega = \frac{\alpha L}{\theta_m V_m}$

$Z = x/L$

Analytical solutions to Equations (8) and (9) are available for various initial and boundary conditions (Lapidus and Amundson, 1952; Van Genuchten and Wierenga, 1976; Van Genuchten, 1981). Using the following initial and boundary conditions expressed in dimensionless variables,

$$C_1 = C_2 = 0 \qquad \text{at } Z > 0 \quad , \quad T = 0 \tag{10}$$

$$\left[-\frac{1}{P}\frac{\partial C_1}{\partial Z} + C_1\right] = 1 \qquad \text{at } Z = 0 \tag{11}$$

$$\frac{\partial C_1}{\partial Z} = 0 \qquad \text{at } Z = \infty \quad , \; T \geq 0 \tag{12}$$

Van Genuchten (1981) expressed the general solution of Equations (8) and (9) for the exit concentration, (Z = 1), as:

$$C_1 = G(T)\, \exp\left|\frac{-\omega T}{\beta R}\right| + \frac{\omega}{R}\int_o^T G(\tau)\, H(T,\tau)\, d\tau \tag{13}$$

where

$$H(T,\tau) = \exp(-a-b)\left[\frac{I_o(\xi)}{\beta} + \frac{\xi I_1(\xi)}{2b(1-\beta)}\right] ,$$

$$a = \frac{\omega\tau}{\beta R};$$

$$b = \frac{\omega(T-\tau)}{(1-\beta)R};$$

$$\xi = 2\sqrt{ab};$$

I_o and I_1 = modified Bessel functions;

and

$$G(\tau) = \left|\frac{1}{2}\,\mathrm{erfc}\left[\left|\frac{P}{4\beta R\tau}\right|^{1/2}\left|\beta R - \tau\right|\right] + \left|\frac{P\tau}{\pi\beta R}\right|^{1/2}\exp\left[\frac{-P}{4\beta R\tau}\left|\beta R+\tau\right|^2\right]\right.$$
$$\left. - \frac{1}{2}\left|1 + P + \frac{P\gamma}{\beta R}\right| \exp(P)\,\mathrm{erfc}\left[\left|\frac{P}{4\beta R\gamma}\right|^{1/2}\left|\beta R + \tau\right|\right]\right|$$

It should be noted that Equation (13) contains four independent parameters; P, β , R, and ω . If there is no sorption, (k=0), R equals one and β reduces to the fraction of the total porosity making up the mobile fluid regions, (θ_m/θ).

The above analytical development provides a model of the leaching process which incorporates a number of transport mechanisms likely to be present. By fitting solutions of this analytical model to actual leaching column test results the adequacy of the model can be tested and the importance of the various transport mechanisms to the dispersion process can be assessed. in the investigation which follows, this is accomplished by fitting analytical solutions for the case where k = 0 (Case I model) and for the case where $k \neq 0$ (Case II model) to a number of leaching column test results. Because the leaching tests were conducted under saturated conditions, it is assumed that the immobile fluid regions, θ_{im}, and the mobile fluid regions, θ_m, are equal to the mediums micro porosity, ϕ_{micro}, and macro porosity, ϕ_{macro}, respectively. In this way, the dimensionless parameters P, β, R, and ω , which will be obtained from the solution of the analytical model, can be compared to the dispersion characteristics they are supposed to represent. Using the definitions of these dimensionless parameters, values of d, f, k, and α can be calculated and likewise compared to their defined role in the dispersion process. Although the actual values of these parameters are not known, variations in the leaching column test conditions can be compared to the variations in the model parameters.

CHAPTER III

LABORATORY PROCEDURES

A. Experimental Design

The leaching column tests conducted in this investigation were designed to test three different particle sizes of the same material at three different pore velocities and at equal leachant residence times. Spent shale from the indirectly heated Paraho retort process was separated into three particle size ranges by dry mechanical sieving. The sieves used and the resulting particle size ranges were:

U.S. Standard Sieves No. 40 and No. 16 ; 0.420 mm - 1.190 mm
U.S. Standard Sieves No. 16 and No. 10 ; 1.190 mm - 2.000 mm
U.S. Standard Sieves No. 8 and No. 6 ; 2.362 mm - 3.327 mm

Columns containing each of these size ranges were leached at three different pore velocities (seepage velocities) for a total of nine leaching tests. In order to easily identify the materials and pore velocities used in the different tests, the particle size ranges are designated A, B, and C, respectively, from smallest to largest, with the pore velocities used for each media designated 1, 2, and 3, respectively, from the smallest to the largest. For example, the leaching column test with the 1.190 mm - 2.000 mm particle size medium conducted at the lowest pore velocity is referred to as test B-1 and the leaching column test with the 2.362 mm - 3.327 mm particle size medium conducted at the highest pore velocity is referred to as test C-3.

The diameters and lengths of the columns were varied from test to test in order to maintain a constant overall fluid residence time at the

various seepage velocities. By doing this the contact time of a given fluid element with a given pore volume element varies according to the prescribed pore velocity, while the average time for this fluid element to travel the overall length of the column is constant.

B. Determination of Porosity

Calculation of the Darcy flow rate through the column that corresponds to a prescribed pore velocity requires knowledge of the porosity through which bulk flow occurs. Since the Paraho residue is bi-modal with respect to porosity and pore size, it is assumed that bulk flow occurs only through the macro pores. It was therefore necessary to identify the micro and macro portions of the total porosity. Calculation of the seepage velocity is based only on the macro porosity, which for this medium is substantially smaller than the total porosity.

A number of tests were used to determine micro, macro, and total porosity. These are:

A. water uptake (release) test which measures the quantity of water gained (lost) through vacuum saturation (oven drying) of a sample of spent shale particles,

B. water displacement test using oven dried spent shale particles.

In the water uptake (release) test, a representative sample of oven dried spent shale (minimum weight of 100 g) with the desired range of particle sizes is placed in a vacuum cylinder and evacuated (~23 inches of Hg vacuum) for a minimum of six hours. A quantity of distilled water sufficient to saturate the sample is added while maintaining a vacuum. The vacuum is then released and the sample is poured onto a fine mesh screen of known weight. The particles are gently spread in order to

facilitate removal of excess water from the exterior of the spent shale particles. Care is taken to ensure that all sample particles are on the screen. When the screen appears to be dry and there is no excess water visible on the exterior of the shale particles, the screen and sample are weighted. The difference between the wet weight and the oven dry weight of the particles represents the weight of water occupying the interconnected micro pores. As a check on previous measurements, the sample is again oven dried to determine the weight loss. Taking the density of water to be 1.0 g/cm^3, the average volume of micro porosity per unit dry weight of spent shale is known. The volume of micro space expressed in this manner is a constant and is independent of the bulk density subsequently achieved in packing the column for leaching.

For the water displacement test, a sample of oven dried shale is placed in a 100 ml cylinder of known weight. An appropriate quantity is that which fills half the cylinder. The cylinder and dry shale are weighed and 50 ml of distilled water is added. A rubber stopper with a vacuum connection is then used to seal the cylinder. The cylinder is evacuated (~23 inches of Hg vacuum) for a minimum of 18 hours, occasionally shaking the cylinder to release trapped air and vapor bubbles. The vacuum is then released and the sample allowed to settle. The levels of the shale and the water are recorded, the stopper is removed, and the graduated cylinder and contents are weighed. The data from this test permit calculation of the apparent particle density. The term 'apparent particle density' is used here due to the fact that the methods utilized do not account for non-interconnected micro pore space. Any non-interconnected micro pore space is included as part of the solid volume, and therefore tends to decrease the particle density. With the apparent

particle density, ρ_p, and the volume of micro space per unit weight, ϕ^{ω}_{micro}, calculated from these tests, the macro porosity, ϕ_{macro}, for any bulk density, ρ, can be easily computed by:

$$\phi_t = 1 - \frac{\rho}{\rho_p} \tag{14}$$

$$\phi_{micro} = \phi^{\omega}_{micro} \times \rho \tag{15}$$

$$\phi_{macro} = \phi_t - \phi_{micro} \tag{16}$$

where: ϕ_t = total porosity = volume of interconnected pores per unit bulk volume (L^3/L^3)

ρ_p = apparent particle density = dry weight of solids per unit volume of solids (M/L^3)

ϕ_{micro} = micro porosity = volume of interconnected micro space per unit bulk volume (L^3/L^3)

ϕ^{ω}_{micro} = volume of interconnected micro space per unit dry weight of solids (L^3/M)

ϕ_{macro} = macro porosity = volume of macro space per unit bulk volume (L^3/L^3)

C. Leaching Procedure

The leaching tests were carried out in Lucite columns with distilled water as the influent. A positive displacement pump was used to cause flow from a constant head intake reservoir to occur upward through the columns. As shown in Figure 5, the effluent flows through an overflow fitting in which the temperature and electrical conductivity probes are fixed. The electrical conductivity and temperature were

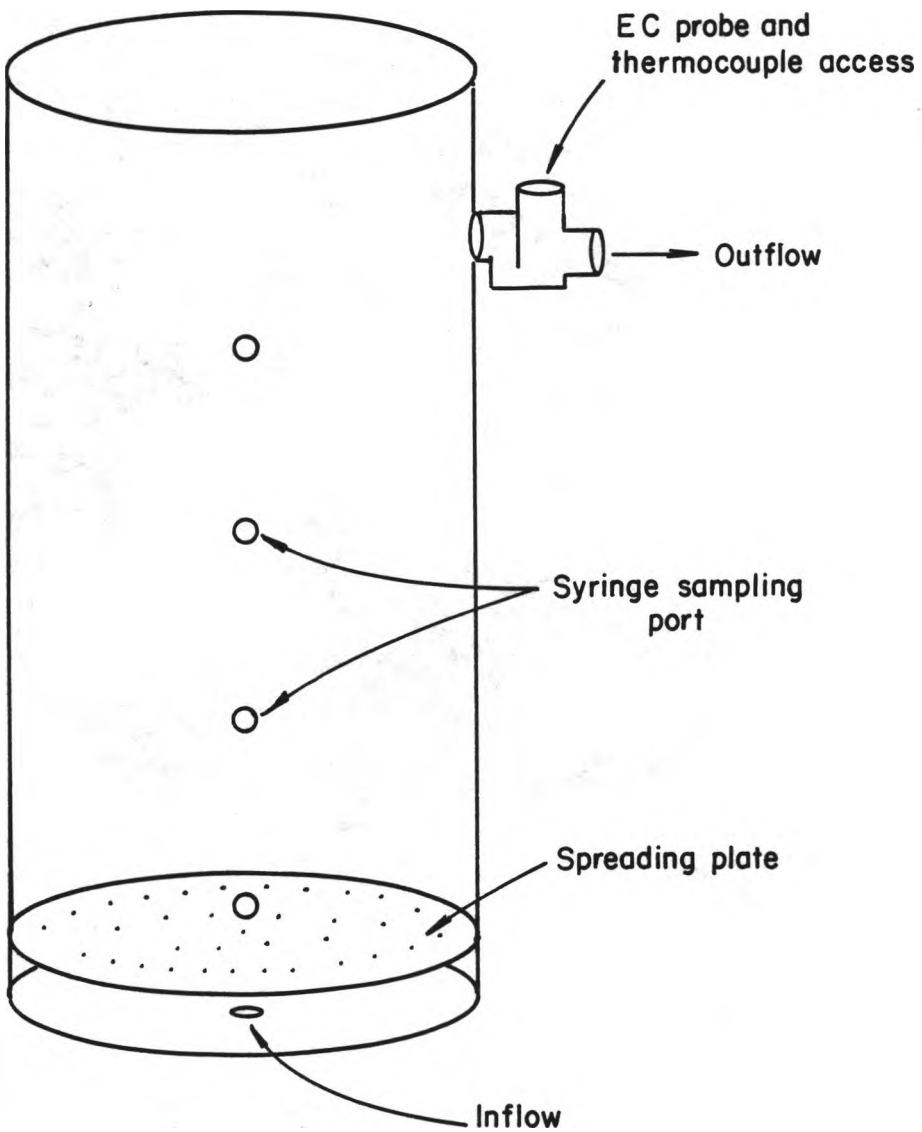

Figure 5. SCHEMATIC DIAGRAM OF LEACHING TEST APPARATUS

automatically logged onto a paper tape at predetermined time intervals. Flow rates were measured by timing the effluent into a 10 ml burrette. An important feature of the column design is the distribution plate placed beneath the shale in the column. The function of this plate is to evenly spread the influent across the column section. Without this distribution plate, channeling of the influent through a small portion of the column section was observed.

To assist in assuring that the influent was properly distributed, dye tracer tests were performed on each column before the shale was added. The columns were filled with tap water and placed under a vacuum to remove air from the distributon plate. A dye was then pumped into the column and up through the distribution plate. If the flow distribution was observed to be uneven, the distribution plate was removed and modified. This testing procedure was repeated until relatively uniform flow distribution was observed. The column was then cleaned and dried in preparation for placement of the shale.

Roughly 3,000 to 4,000 grams of spent shale were used in each leaching test, depending on the volume of the cylinder used and the bulk density achieved. The material was added to the columns through a funnel with a long stem in four lifts, so that approximate uniform bulk density was achieved. Some compaction was obtained by gently tapping the exterior of the column. Once the shale had been packed to the elevation of the overflow fitting, the column was sealed using a stopper in the overflow fitting and a lid with an O-ring on the top. The column was then evacuated for a minimum of 24 hours.

A sample of approximately 500 g of the spent shale was weighed and oven dried to determine the moisture content of the medium so that the

dry bulk density could be determined. Following evacuation for 24 hours or more, deareated distilled water was allowed to slowly enter the column through the inlet port at the bottom of the column. Typically about four hours were required to bring the fluid level to the top of the shale. Once the fluid level reached the top of the shale, the vacuum was alternately released and applied until all vapor and entrapped air bubbles were eliminated. Some settling of the solids was observed. In such cases, the bulk density was recalculated and additional shale added to bring the level to that of the overflow fitting at that density. Vacuum saturation was repeated and a final bulk density computed.

The columns were allowed to rest undisturbed for a minimum of seven days to allow the pore fluid time to reach chemical equilibrium with the spent shale media. Following the equilibration period, fluid samples were withdrawn from the column through the syringe ports (see Figure 5) and the electrical conductivity determined. The sample was then placed back into the column at the top. This process was repeated daily until the EC readings showed little variation with time or position in the columns.

When it was determined that chemical equilibrium had been achieved (at least insofar as a stable EC indicates chemical equilibrium), the leaching test was initiated. The suction line for the pump was placed in the distilled water reservoir and the pump turned on to fill the suction and discharge tubing. The discharge tubing was then connected to the column inlet port and the valve opened. The effluent discharge was measured by timing the flow into a burrette, and EC and temperature measurements were automatically taken and recorded every 15 minutes.

The EC measured by the probe was periodically checked against a standard, and independent determinations were occasionally made on samples of the effluent. The leaching tests were continued until the EC readings reduced to an approximate constant value.

D. NaCl Leaching Test

In an attempt to gain insight into the effects of diffusion into (and out of) the micro pore space versus the effects of chemical reaction and sorption, one column was subjected to additional tests. After completing the previously described leaching test on one of the Media B columns, the influent was switched to a prepared solution of NaCl with an EC of about 7,300 μ mhos/cm. After breakthrough occurred and the EC of the effluent stabilized to approximately that of the influent, the influent source was again switched to distilled water. The test was continued until the effluent EC readings were again reduced to approximate constant values.

CHAPTER IV

LABORATORY RESULTS

A. Determination of Porosity

It was expected in the water uptake test that there would be an easily recognized point during the draining of the spent shale particles at which excess water on the exterior of the particles had drained, yet water in the micro pore space had not. In practice, however, this was not the case. Instead, there seemed to be a range of moisture content values during which this condition could be judged to occur. This range extended roughly from $\phi^{\omega}_{micro} = 0.28$ cm^3/g soon after spreading the shale on the screen (the particles were obviously wet and clumped together), to $\phi^{\omega}_{micro} = 0.16$ cm^3/g (the particles were dry, no moisture visible on the particle surfaces). This range appeared to be the same for the three particle sizes tested, although the largest particles (medium C) drained much more quickly than the smaller particles (mediums A and B). To aid in selecting a particular value of ϕ^{ω}_{micro} within this range, a small sample of medium A size particles having an initial saturated water content of about 0.24 cm^3/g was viewed under a microscope. Evaporation aided by heat from the microscope lamp dried these particles in a short time. Observations showed that water did not cover the entire surface area of the particles, but instead appeared as small droplets scattered on the surface. There was no observable miniscus formed at the junction of two particles. As the particles dried, the water dro-

plets on the surface decreased in size but were present long after the particles appeared completely dry to the naked eye. It was believed that the absence of a liquid covering or a miniscus at particle junctions indicated that a moisture content closer to the initial value of 0.24 cm^3/g would be a better estimate of ϕ^{ω}_{micro} than values at the lower end of the range. Also, porosity calculations performed using selected values of ϕ^{ω}_{micro} at the lower end of the range gave unreasonably high values for ϕ_{macro}. Table 1 lists the values of ϕ_{macro} calculated for the nine leaching column tests for a range of values of ϕ^{ω}_{micro}. For the compaction achieved in packing these columns it is felt that values for macro porosity should be within the range of 0.35 to 0.45. For these reasons, a value of $\phi^{\omega}_{micro} = 0.22$ cm^3/g was chosen for use in the porosity calculation for all three particle size ranges.

Table 1. Computed Values of Macro Porosity for Selected Values of ϕ^{ω}_{micro}, assuming $\rho_p = 2.608$ g/cm^3

Leaching column Test	ϕ^{ω}_{micro} 0.16	ϕ^{ω}_{micro} 0.19	ϕ^{ω}_{micro} 0.22	ϕ^{ω}_{micro} 0.25	ϕ^{ω}_{micro} 0.28
A-1	0.4358	0.4046	0.3735	0.3424	0.3112
A-2	0.4362	0.4051	0.3739	0.3428	0.3117
A-3	0.4303	0.3998	0.3674	0.3359	0.3044
B-1	0.4165	0.3843	0.3521	0.3199	0.2877
B-2	0.4868	0.4585	0.4302	0.4018	0.3735
B-3	0.4339	0.4027	0.3714	0.3402	0.3089
C-1	0.4980	0.4703	0.4426	0.4149	0.3871
C-2	0.4161	0.3838	0.3516	0.3194	0.2871
C-3	0.4266	0.3949	0.3632	0.3316	0.2999

Three water displacement tests gave values for ρ_p of 2.602 g/cm^3, 2.589 g/cm^3, and 2.633 g/cm^3. Particle size is not expected to have any effect on the value of ρ_p, although due to the testing methods used, the presence of non-interconnected pore space would tend to decrease the computed value of ρ_p. If non-interconnected pore space is present, the effect would be expected to be most noticable with the larger particle size. This was not observed in the tests run, and in fact, the highest particle density was calculated for the largest grain size. An average value of ρ_p = 2.608 g/cm^3 was therefore used in the porosity calculations.

The results of the porosity calculations using these estimates of ϕ^{ω}_{micro} and ρ_p are listed in Table 2.

Table 2. Porosity Calculations Using Estimates of ρ_p = 2.608 g/cm^3 and ϕ^{ω}_{micro} = 0.22 (cm^3/g)

Leaching Test	Dry Bulk Density ρ_β (g/cm^3)	Total Porosity ϕ_t	Micro Porosity ϕ_{micro}	Macro Porosity ϕ_{macro}
A - 1	1.0382	0.6019	0.2284	0.3735
A - 2	1.0375	0.6022	0.2283	0.3739
A - 3	1.0484	0.5980	0.2306	0.3674
B - 1	1.0737	0.5883	0.2362	0.3521
B - 2	0.9443	0.6379	0.2077	0.4302
B - 3	1.0417	0.6006	0.2292	0.3714
C - 1	0.9238	0.6458	0.2032	0.4426
C - 2	1.0746	0.5880	0.2364	0.3516
C - 3	1.0553	0.5954	0.2322	0.3632

B. Leaching Tests

The electrical conductivity data collected during each leaching test were adjusted to a temperature of 25°C and normalized by dividing the values by the highest value recorded during the test. Pore volume calculations for each leaching test were accomplished using the macro porosity values determined previously and the average of the flow rate measurements according to:

$$\text{PORE VOLUMES} = \frac{Q\ t}{A\ L\ \phi_{macro}}$$

where

Q = average flow rate, (L^3/T)

t = elapsed time from the start of the leaching test, (T)

A = area of column, (L^2)

L = length of column, (L)

As a matter of convention for comparison purposes, it was decided to plot all breakthrough curves in terms of the normalized tracer concentration in the displacing (influent) fluid. This allowed for the use of Equations (10) (11) and (12) as the initial and boundary conditions used in solving the modified dispersion equation. The measured normalized concentrations were therefore subtracted from 1.0 to arrive at the normalized displacing fluid concentrations. Plots of the normalized breakthrough curves for the nine leaching tests conducted are shown in Figures 6, 7, and 8.

Normalized breakthrough curves were also produced for the two NaCl leaching tests (see Figure 9). These are also plotted in terms of the displacing fluid tracer concentration. Unlike the other leaching tests,

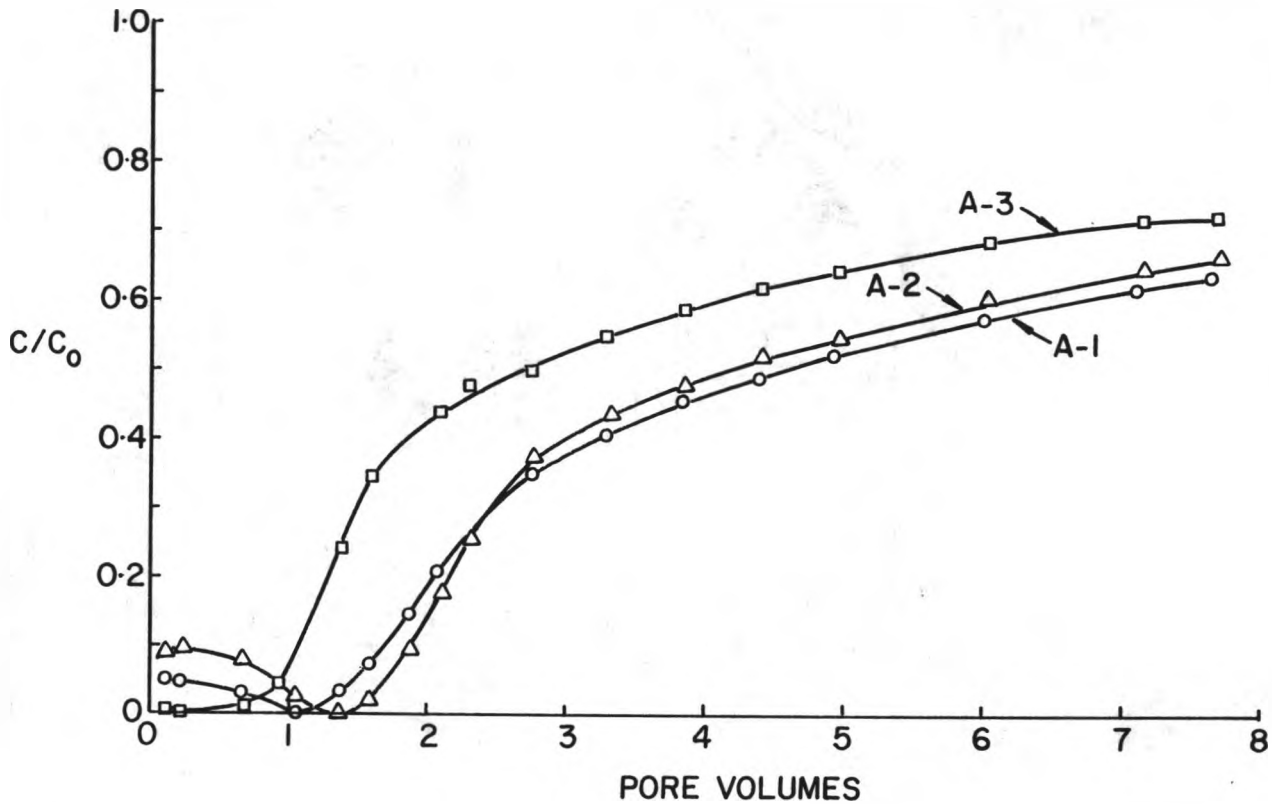

Figure 6. NORMALIZED BREAKTHROUGH CURVE FOR 0.420 - 1.90 mm GRAIN SIZE PARAHO SPENT SHALE MEDIA

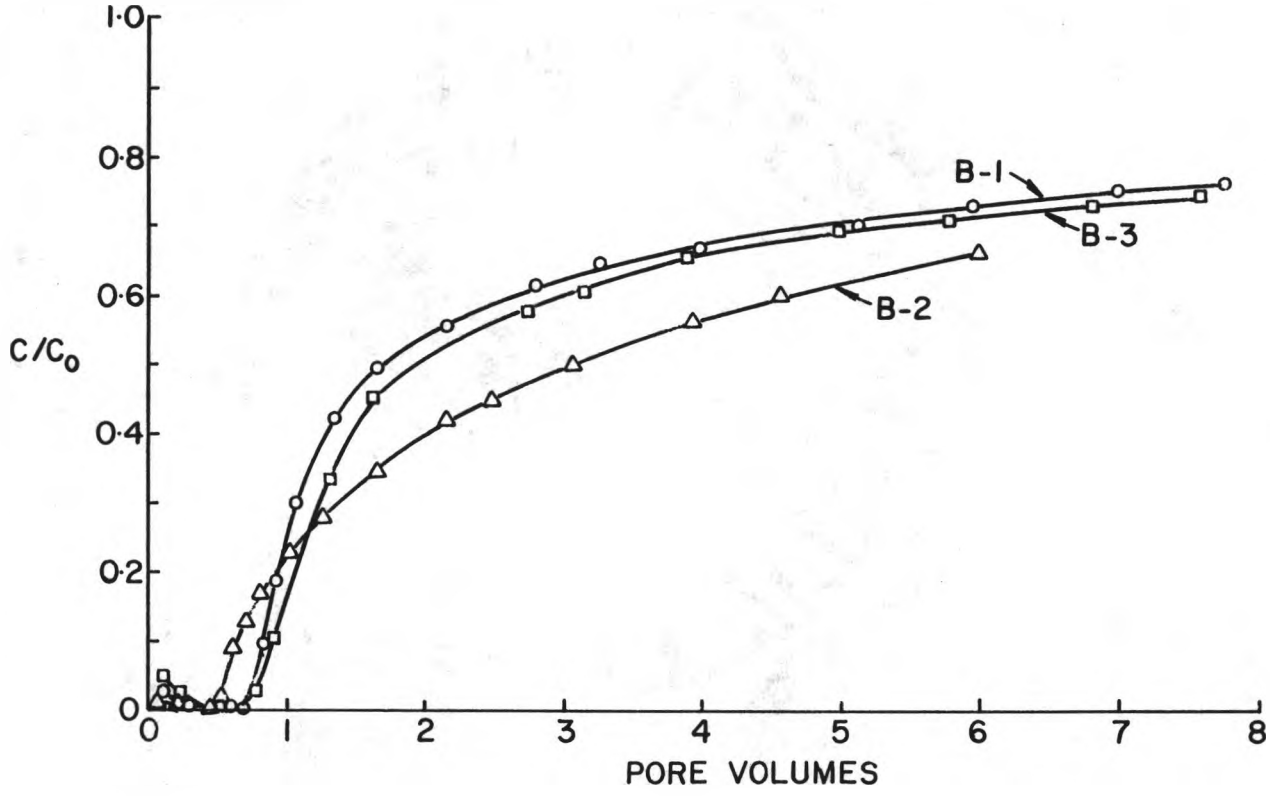

Figure 7. NORMALIZED BREAKTHROUGH CURVES FOR 1.90 - 2.000 mm GRAIN SIZE PARAHO SPENT SHALE MEDIA

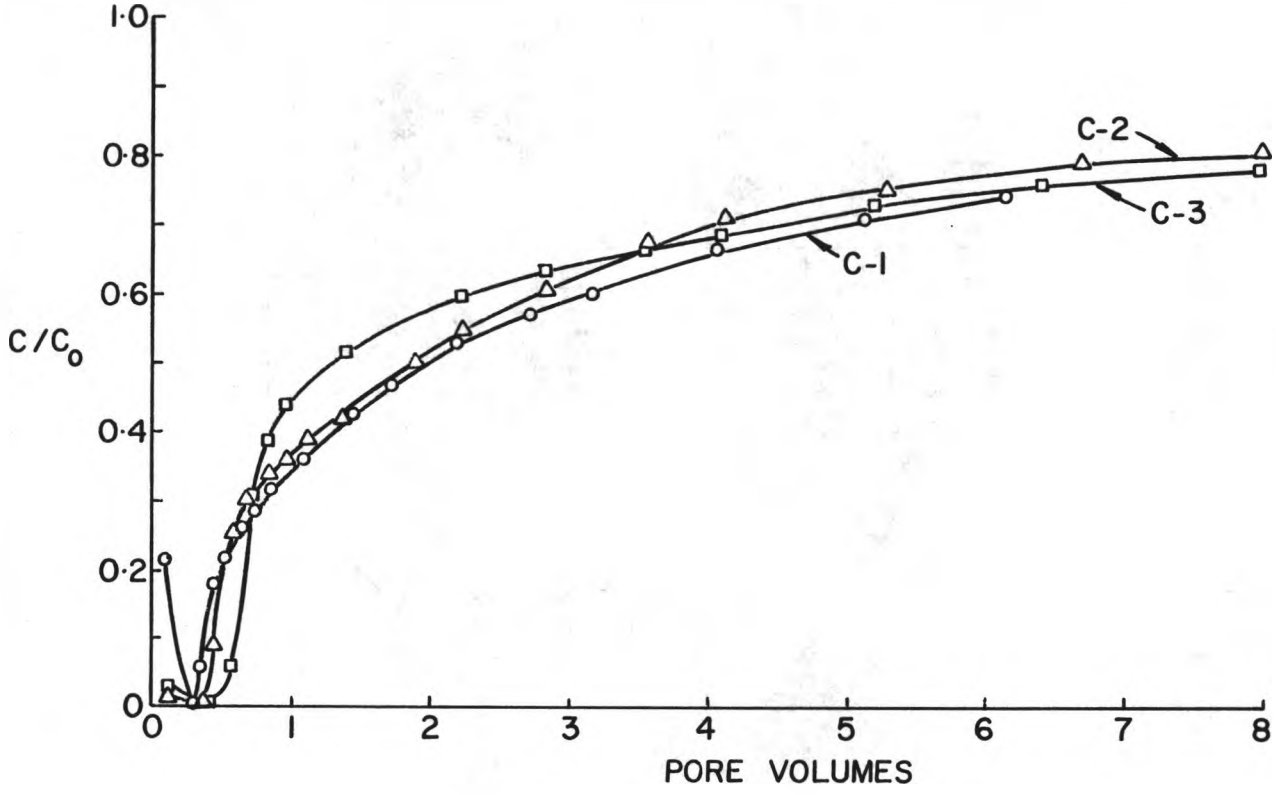

Figure 8. NORMALIZED BREAKTHROUGH CURVES FOR 2.362 - 3.327 mm GRAIN SIZE PARAHO SPENT SHALE MEDIA

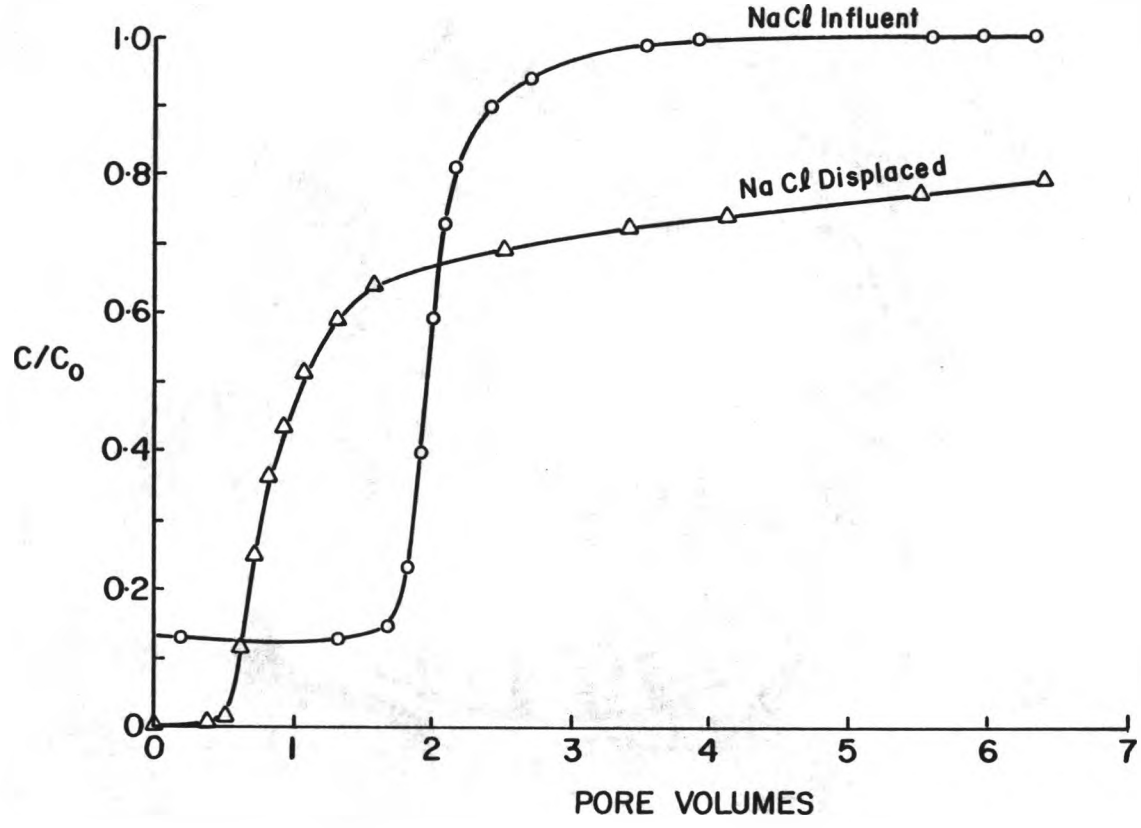

Figure 9. NORMALIZED NaCl BREAKTHROUGH CURVES USING LEACHED 1.190 - 2.000 mm GRAIN SIZE PARAHO SPENT SHALE MEDIA

the tracer concentration measurements in the NaCl leaching tests were complicated by a background electrical conductivity caused by continued contribution from the spent shale. Although the EC of the NaCl tracer solution and the background EC of the displaced fluid could be measured separately, it was found that the EC was not additive when the fluids were combined. Correction of the tracer measurements could therefore not be made by subtracting a value for the background EC. Because of this, the NaCl breakthrough curves shown in Figure 8 include the effects of the background EC.

Information on the system parameters for the nine leaching column tests and two NaCl leaching tests is listed in Table 3. The pore velocities (seepage velocities) and fluid residence times were computed as follows:

$$V_s = \frac{Q}{A\ \phi_{macro}} \tag{17}$$

$$D_t = \frac{A\ L\ \phi_{macro}}{Q} \tag{18}$$

where:

V_s = seepage velocity, (L/T)

D_t = fluid residence time, (T)

Table 3. Leaching Test Parameters

Leaching Test	A (cm^2)	L (cm)	Q (cm^3/hr)	V_s (cm/hr)	D_t (hrs)
A - 1	114.326	28.0	130.47	3.055	9.164
A - 2	84.970	37.7	131.69	4.145	9.095
A - 3	84.970	48.0	164.41	5.267	9.114
B - 1	114.326	28.0	121.94	3.029	9.243
B - 2	84.970	38.4	116.75	3.194	12.023
B - 3	80.870	48.3	152.74	5.085	9.498
C - 1	114.326	27.0	116.75	2.307	11.702
C - 2	80.870	39.6	125.61	4.418	8.964
C - 3	84.970	47.7	163.67	5.303	8.994
NaCl influent	84.970	38.4	131.12	3.587	10.705
NaCl displaced	84.970	38.4	131.39	3.594	10.683

CHAPTER V

DATA ANALYSIS AND DISCUSSION

A. Computer Analysis

To help analyze and compare the leaching column test results, a least-squares curve fitting computer model developed by Van Genuchten (1981) was used. This model (CFITIM) calculates the unknown parameters of Equations (8) and (9) on the basis of a least-squares curve fit of leaching column effluent data. It also calculates a 95 percent confidence interval for each unknown parameter and the exit concentrations for the analytical solution corresponding to the test results used as input. A description of the computer program and a program listing can be found in Appendix A.

To use the program, points were selected from each set of breakthrough data. The program requires that initial estimates for P, R, β , and ω be made. If the value of any of these paraamaeters is known, that value can be held constant. The program makes iterative selections of the unknown parameters until the relative change in the ratio of the parameters becomes less than a predetermined value. In these calculations a value of 0.0005 was used.

In analyzing the test data two cases were considered:

Case I: Asymmetry of the breakthrough curve is assumed to be caused only by the bi-modal property of the media. No sorption process is present in this case; therefore, R = 1.0 and β reduces

to θ_m/θ which in these leaching tests is assumed equal to ϕ_{macro}/ϕ_t. This leaves P and ω as the only unknown parameters.

Case II: Asymetry of the breakthrough curve is assumed to be caused by both the bi-modal property of the media and a linear sorption process. In this case P, R, β, and ω are all unknown parameters. It should be emphasized that by assuming a linear sorption process to be present, the model will force the other processes to conform to this description. Values obtained for the models' parameters in this manner may not correlate with the defined physical significance of the parameters if processes other than linear sorption play a significant role in the tracers' dispersion.

In both cases, the initial and boundary conditions used were equations (10), (11) and (12).

For Case I, the computer calculated iterative values of ω which continually vascilated by as much as 1,000 and failed to converge on a specific value. Also, plots of the analytical breakthrough curves produced after 20 iterations did not match the test data very well. Because of this, the Case I analytical model was considered inadequate for explaining the asymmetry of the breakthrough curves. Emphasis of the study was therefore switched to Case II.

The analytical solutions for Case II did converge on values for P, R, β, and ω, and produced breakthrough curves which were very close to the actual laboratory results. As an example, a plot of the measured breakthrough curve for leaching test A-3 is shown in Figure 10, along with the computer generated exit concentrations produced for Case I and

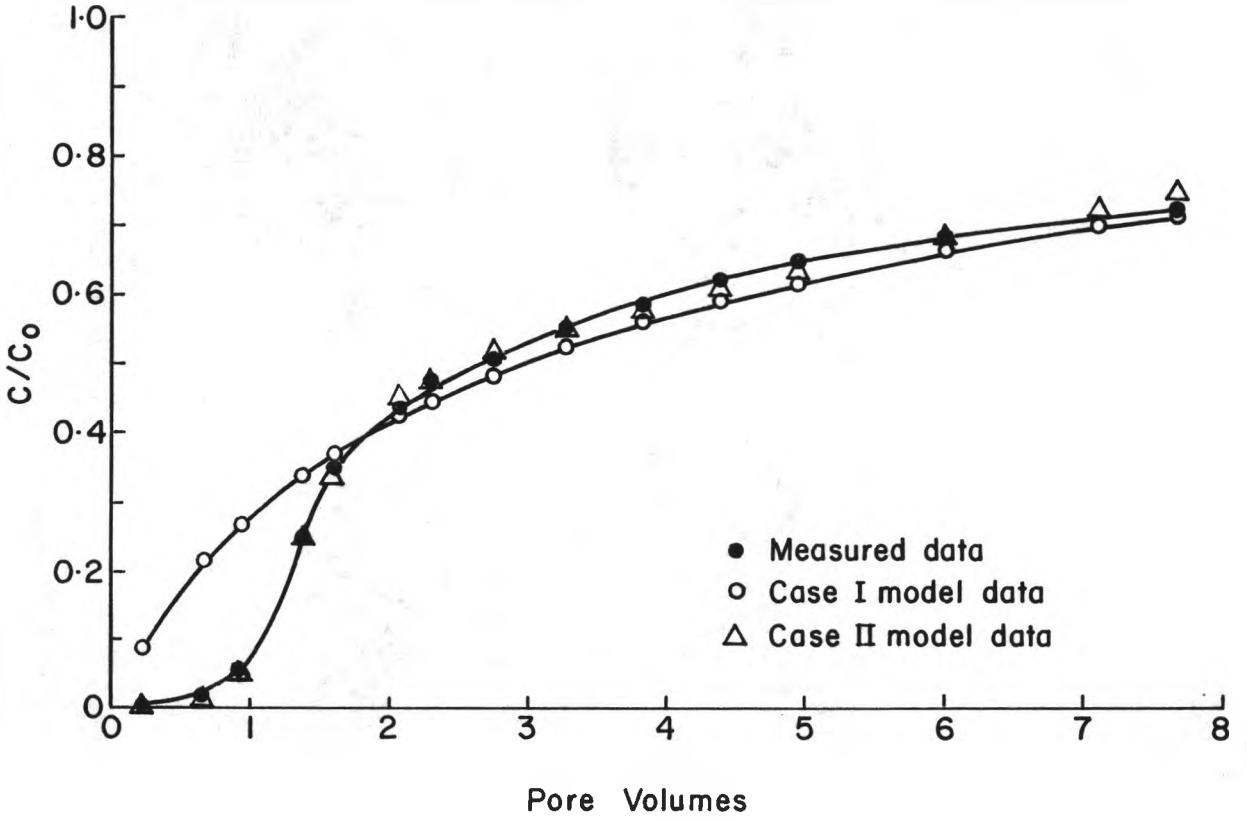

Figure 10. COMPARISON OF LEACHING TEST A-3 BREAKTHROUGH CURVE TO CASE I AND CASE II COMPUTER MATCHED CURVES

Case II. A curve is not drawn through the Case II data points since it would obscure the measured breakthrough curve.

Another example, (leaching test C-2), is shown in Figure 11 to illustrate the worst agreement obtained between the actual laboratory exit concentrations and those of the Case II analytical solution.

The values of P, R, β, and ω calculated using the Case II model are listed in Table 4 for the nine spent shale leaching tests and the displaced NaCl leaching test. No analysis of the NaCl influent leaching test was done due to the complications caused by the background electrical conductivity levels. Using the dimensionless variable relationships, values of D, f, k, and α were calculated and are listed in Table 5.

Table 4. Summary of Dimensionless Parameters Calculated by CFITIM

Leaching Test	P	R	β	ω
A - 1	19.05178	7.51485	0.29493	0.98867
A - 2	45.79022	7.21596	0.31006	0.96723
A - 3	19.84306	5.53263	0.25884	0.81221
B - 1	20.95618	4.97345	0.22297	0.64679
B - 2	7.56161	4.79277	0.22365	1.13981
B - 3	18.47980	5.43902	0.23633	0.61856
C - 1	7.45016	3.53312	0.16813	1.08712
C - 2	66.91943	3.57700	0.14593	1.14892
C - 3	33.00896	4.40281	0.16217	0.70712
NaCl displaced	19.32578	3.86341	0.21349	0.48252

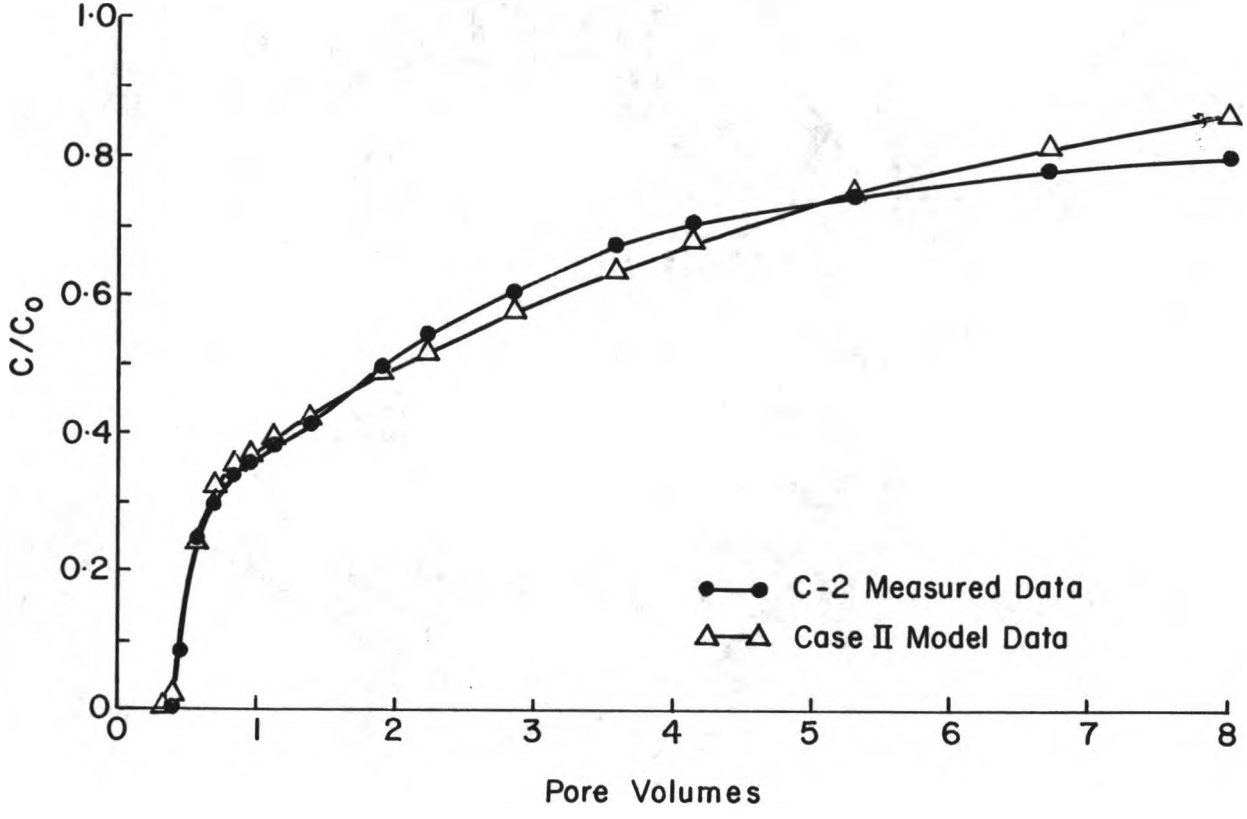

Figure 11. ILLUSTRATION OF THE WORST CASE II COMPUTER MATCHED BREAKTHROUGH CURVE OBTAINED

Table 5. Summary of Transport Model Coefficients Calculated from the Dimensionless Parameter Values

Leaching Test	Dispersion Coefficient D (cm/sec)	Fraction of Solid in Contact with Mobile Liquid f	Sorption Rate Constant k (cm^3/g)	Diffusional Rate Constant α (sec^{-1})
A - 1	1.2472×10^{-3}	0.24495	3.77701	1.1192×10^{-5}
A - 2	9.4797×10^{-4}	0.26005	3.60795	1.1045×10^{-5}
A - 3	3.5392×10^{-3}	0.18040	2.58538	9.0957×10^{-6}
B - 1	1.1242×10^{-3}	0.12846	2.17713	6.8433×10^{-6}
B - 2	4.5056×10^{-3}	0.10481	2.56212	1.1329×10^{-5}
B - 3	3.6918×10^{-3}	0.15026	2.55935	6.7184×10^{-6}
C - 1	2.3224×10^{-3}	-.03605	1.77083	1.1420×10^{-5}
C - 2	7.2620×10^{-4}	-.02948	1.41008	1.2519×10^{-5}
C - 3	2.1287×10^{-3}	0.03056	1.91986	7.9315×10^{-6}
NaCl displaced	1.9837×10^{-3}	0.05252	1.93431	5.3968×10^{-6}

B. Discussion of Results

As suggested previously, there exists no standard procedure for conducting column leach tests. The relationship of total dissolved solids and chemical composition in effluent to elapsed leaching time depends upon throughput rate, length of column, and the manner in which the leachant is introduced, among other factors. Meaningful interpretation and comparison of results is enhanced if basic parameters of the leaching process, which are independent of column length and throughput rate, can be identified and evaluated. One method of approach is to formulate a mathematical model that includes the relevant parameters,

conduct the leaching test so that the requisite boundary and initial conditions are satisfied, and determine the unknown parameters in the model by adjusting the parameters until there is agreement between the measured and calculated results.

The leaching procedure used in this study was adopted with the intent of establishing initial, boundary, and flow conditions that are convenient for mathematical analysis. Of the various mathematical models that could be utilized, it appeared that the Van Genuchten-Wierenga model (Eqs. 6 and 7) incorporates more of the fundamental processes that might be expected to affect the leaching phenomenon. Before proceeding to a discussion of the results obtained using this model, several comments concerning the relevance of this model to the leaching process are in order.

The intended application of the Van Genuchten-Wierenga model was to problems of transport of a particular contaminant introduced into the porous medium with influent water. Included in the transport model are parameters that account for adsorption of the contaminant on the exchange complex and diffusion into regions containing essentially immobile pore fluid. A zero concentration of contaminant in the pore liquid at t=0 is the appropriate initial condition for such an application. In contrast, the leaching process is one of removal of chemical species resident in the column at the initiation of leaching. The concentration of various species in the pore liquid at the end of the equilibration period is supposed to be uniform so a simple transformation accomodates the obvious difference in initial condition.

Production of particular chemical species into the flowing fluid during leaching is supposed to result from desorption of adsorbed ions,

diffusion from regions of immobile solution, and dissolution of the mineral solids. Locally, these mechanisms can be operating in either direction for a particular species and are affected by the total concentration and composition of solution. Sorption processes are included in the Van Genuchten-Wierenga model via a linear isotherm. While a linear isotherm model may be adequate in some applications, it can be expected to be no more than a rough approximation for individual ions in the complex solution present in the pore solution of the leaching columns. Furthermore, the isotherm constant for different cations is undoubtedly different.

Transfer of individual ions between the regions of mobile and immobile fluid by diffusion is modeled in the Van Genuchten-Wierenga formulation by assuming the transfer rate is proportional to the difference in concentration between the two regions. The proportionality constant (α in Equation 7) and the difference in concentration is expected to depend upon which species is under consideration in a complex, multispecies system such as the leaching columns.

Dissolution and precipitation is not explicitly accounted for in the Van Genuchten-Wierenga model. Chemical dissolution and precipitation are thought to be heterogeneous chemical reactions that occur in three steps; transfer of reactants to the reaction site, the chemical reaction itself, and transfer of reaction products away from the site. The overall reaction rate is controlled by the slowest of these steps. If it is assumed that the transfer process is the rate controlling step, then the diffusion mechanism already present in the model could be regarded as a model for the rate dependent chemical reactions.

Diffusion path length and concentration differences appropriate for the chemical reaction are different than for diffusonal transfer between the micro and macro pore regions, however.

It would be possible to determine the concentration of individual species in the column effluent and calculate therefrom values for the coefficients of hydrodynamic disperson, the isotherm constant k, and the diffusional transfer parameter α that correspond to individual species. The values so obtained would be, at best, effective values reflecting some average affected by other species in an unknown way. At worst, the values might have little or no physical relevance.

The question of physical significance of parameters obtained for individual species by fitting the model to effluent data led the author to focus attention on the electrical conductivity of the effluent. An objective of the study was to assess the suitability of the previously described leaching procedure in terms of consistency and comparability. Even though the EC carries little chemical information, it is readily measured and thought to be an adequate effluent characteristic for the purposes of this study. All results are analyzed in terms of ratios of EC. Ratios of concentration referred to in the following paragraphs and elsewhere are actually ratios of EC. Determination of the leaching parameters D, k, and α made by fitting the Van Genuchten-Wierenga model to effluent EC data was done to assist in assessing the suitability of the leaching technique. In this context, the parameters are curve fitting parameters with limited physical significance.

In viewing the breakthrough curves in Figures 6, 7, 8, and 9 several interesting properties are observed. All of the nine spent shale leaching tests showed an initial variation in tracer concentration

which could not be explained by monitoring probe error. This variation shows up in the normalized breakthrough curve as a gradual decrease in concentration from an initial positive value to the point $C/C_o = 0$ just before breakthrough began. In terms of the actual tracer readings, this means that the electrical conductivity readings gradually increased to a peak value just before the breakthrough front passed. Syringe samples of resident fluid in the columns showed no EC gradient through the length of the column prior to initiation of leaching; the reason for this is thought to be a small source of low EC water at or near the column overflow. When the leaching tests are started, the displaced higher EC leachate would mix with this low EC water and gradually raise its EC.

The maximum EC reading occurred just before the breakthrough front reached this source of low EC water. The source of this low EC water was at first thought to be either ponded water on top of the media or stagnant water trapped in the overflow fitting. It was believed that small amounts of water in these situations would have lower salt concentrations than the resident fluids in the media since they were not in contact with the media as intimately. Later tests disproved these explanations when this concentration variation still showed up even though excess media was added to eliminate ponded water and the overflow fitting was carefully drained before beginning the test. It is now thought that exposure of the tops of the media to the atmosphere aerated a small layer of resident fluid which caused the EC near the top of the column to be reduced relative to that at depth. This hypothesis has not been tested for confirmation. In the analysis, data points to the left of $C/C_o = 0$ were ignored.

The nine spent shale leaching tests all produced similarly shaped breakthrough curves with a very pronounced tailing effect. There does not appear to be any consistent change in the curves due to seepage velocity, but there is a noticeable retardation of the curves with decreasing media particle size. This is the same effect which Biggar and Nielson (1962) reported in the literature. They attributed this breakthrough curve translation to an increasing size of the macro pores with increasing particle size. Larger macro pores would not mix the tracer as quickly as smaller macro pores thereby allowing the tracer to pass through the media sooner. The physical mixing of tracer is characterized in the Case II analytical solution by the Peclet number, P, which in turn depends on the dispersion coefficient, D. There does not seem to be any consistent change in these values with increasing particle size.

Another explanation for this translation of the breakthrough curve could have to do with the differences in surface area and/or the number and lengths of micro pores between different sized particles. A smaller particle sized media would have a larger surface area exposed to the mobile fluid, and could have a larger number of micro pores with shorter pore lengths. This can be visualized by splitting a particle of one unit volume having a given porosity. The two particles thus formed would have a combined outside surface area which is larger than that of the particle before it was split. Pores which are severed by the split would now be shorter than before and would be exposed to the exterior at two additional locations.

The larger exposed surface area of smaller particles allows for a larger number of sorption sites exposed to the mobile fluid. With more

sites available, more tracer can be transfered to the mobile fluid by this mechanism. No change in the exit tracer concentration would be noticed until the tracer mass depletion due to displacement and mixture with the displacing fluid exceeds the mass addition of tracer due to desorption. This property is modeled in the Case II analytical solution by the dimensionless parameters R and β, which in turn depend on the fraction of solid in contact with the mobile fluid, f, and the sorption rate constant, k. In the computer analysis of the leaching tests, all of these parameters showed a consistent increase with decreasing particle size. Of special note, however, are the values computed for f, the fraction of sorption sites in contact with the mobile fluid. For the largest particle size media, (2.362 - 3.327 mm) the values of f ranged from 0.03056 to -0.03605. Negative values make no sense within the physical definition of this parameter.

The increased number of micro pores and shorter micro pore pathways expected in a smaller particle size media would allow tracer diffusion from the micro pore to the macro pore space to occur more quickly, even though the mass of tracer per unit volume available in the micro pore space would be the same. Again, no change in the exit tracer concentration would occur until the tracer mass depletion due to displacement and mixing exceeds the mass addition of tracer due to diffusion from the micro pores. This property is characterized in both the Case I and Case II analytical solutions by the dimensionless parameter ω, which in turn depends on the diffusional rate constant α. There does not appear to be any correlation of the computed values of these parameters with particle size. The fact that the Case I analytical solution was unable to converge on specific values of ω and that values of ω produced by the Case

II analytical solution did not correlate with particle size, indicates that this mechanism, as modeled, does not play an important role in causing the observed shift in the breakthrough curves.

In contrast to the fresh spent shale leaching tests, the NaCl displacement leaching test produced a breakthrough curve which rises more rapidly, although there is still a pronounced tailing effect. Since the media used in the NaCl leaching test is the same as that used in leaching test B-2, the tracer transfer mechanisms, due to the physical size and shape of the media particles, should be the same. Changes in the shape of the breakthrough curve, therefore, should only be due to differences in chemical transfer mechanisms. There is also a significant difference in breakthrough curves depending on whether the NaCl solution is the displacing fluid or the fluid being displaced. The breakthrough curve produced using the NaCl solution as influent is clearly displaced (retarded) by almost one macro pore volume compared to the curve produced when the NaCl solution was displaced by distilled water. The NaCl influent breakthrough curve is also more symmetrical than the NaCl displaced curve, although some tailing is still present. The displacement of a breakthrough curve to the right is generally explained by adsorption. Adsorption completely removes the tracer from the displacing fluid as long as there are sorption sites available. When all the sorption sites are used up, tracer breakthrough can proceed, effected only by the other transfer mechanisms which are present (i.e. mechanical mixing, diffusion in the macro pores, diffusion into the micro pores). The reverse process of displacing the tracer solution does not necessarily follow the same path since the reverse

transfer mechanisms can differ. Although the NaCl leaching tests conducted were not designed to do so, similar tests could possibly be used to differentiate and quantify these mechanisms.

CHAPTER VI

SUMMARY, CONCLUSIONS, AND RECOMMENDATIONS

In this study, leaching column tests were conducted using spent oil shale medias which exhibited a bi-modal porosity. Breakthrough curves produced from these tests were compared with an analytical model by means of a least squares curve fitting computer model, CFITIM, developed by Van Genuchten, (1981).

It was found that micro pore diffusion, as modeled, could not fully explain the observed asymmetry of laboratory breakthrough curves. When a linear sorption mechanism was coupled with a micro pore diffusion mechanism in the analytical model, a much better match of the breakthrough data was obtained.

Because the model was able to match the breakthrough data, it may be possible to use this analytical model as a standard method of comparing leaching test data. It should be emphasized, however, that since a curve fitting technique was used to match the model to the data, the independent parameters used in the model may not retain the physical significance given to them in developing the model. One indication that this is the case is the fact that some of the computed values for the parameter, f (the fraction of sorption sites in contact with the mobile fluid), are negative. Physically it is impossible to have a negative value for f.

Recognizing the limitations of the CFITIM least squares curve fitting computer analysis, the following conclusions can be drawn.

1. Diffusion of a tracer from a mediums micro pore space to leaching waters as modeled in Equations (3) and (4) does not adequately explain the observed asymmetry of leaching column breakthrough curves.
2. The dispersion model presented in Equations (8) and (9) can be used to fit the observed asymetrical breakthrough curves. The CFITIM curve fitting computer program, which uses this dispersion model, has the potential to be used with a standardized leaching test procedure to compare tracer breakthrough test results.

In order to extend the understanding of the dispersion process to the point where large scale predictions of tracer concentrations can be made, further investigation is needed to define the roles played by the various transport mechanisms. The dispersion model presented in Equations 8 and 9, and the results of this study, provide a starting point to accomplish this. It is recommended that additional testing of the individual transport mechanisms be conducted to see that they are properly defined. Once the proper transport mechanisms are identified and defined, field scale dispersion studies should be conducted to verify the dispersion model.

REFERENCES

Baker, L. E. 1977. Effects of dispersion and dead-end pore volume in miscible flooding. J. Soc. Pet. Engr. 17(3):219-227.

Biggar, J. W. and D. R. Nielsen. 1962. Miscible displacement: II. Behavior of tracers. Soil Sci. Soc. Proc. 26:125-128.

Brigham, W. E. 1974. Mixing equations in short laboratory cores. J. Soc. Pet. Engr. 14(2):91-99.

Coats, K. H. and B. D. Smith. 1964. Dead-end pore volume and dispersion in porous media. J. Soc. Pet. Engr. 4(3):73-84.

Duncan, D. C. and V. E. Swanson. 1965. Organic-Rich Shale of the United States and World Land Areas. U.S. Geological Survey Circular 523.

Goodknight, R. C., W. A. Klikoff and I. Fatt. 1960. Non-steady state fluid flow and diffusion in porous media containing dead-end pore volume. J. Phys. Chem. 64:1162-1168.

Grisak, G. E. and J. F. Pickens. 1980. Solute transport through fractured media: 1. The effect of matrix diffusion. Water Resources Research. 16(4):719-730.

Lapidus, L. and N. R. Amundson. 1952. Mathematics of adsorption in beds. J. Phys. Chem. 56:984-988.

McWhorter, D. B. 1980. Reconnaissance Study of Leachate from Raw Mined Oil Shale-Laboratory Columns: EPA 600/7-80-181, NTIS PB 81 1290 17.

Nielsen, D. R. and J. W. Biggar. 1962. Miscible displacement: III. Theoretical considerations. Soil Sci. Soc. Proc. 26:216-221.

Philip, J. R. 1968. Diffusion, dead-end pores and linearized absorption in aggregated media. Aust. J. Soil Res. 6:21-30.

Turner, G. A. 1957. The flow structure in packed beds. Chem. Engr. Sci. 7:156-165.

USEPA. 1979. Pollution Control Guidance for Oil Shale Development, Revised Draft Report, EPA Oil Shale Work Group, Industrial Environmental Research Laboratory, Office of Research and Development.

Van Genuchten, M. Th. and P. J. Wierenga. 1976. Mass transfer studies in sorbing porous media: I. Analytical solutions. Amer. J. Soil Sci. Soc. 40(4):473-480.

Van Genuchten, M. Th. 1981. Non-Equilibrium Transport Parameters from Miscible Displacement Experiments. USDA Research Report No. 119.

APPENDIX A. CFITIM Computer Program Listing

Table A-1. List of the most significant variables in CFITIM. (From USDA Research Report No. 119, Van Genuchten, February 1981.)

Variable	Definition
B(I)	Vector containing estimates of the various coefficients: P, R and T_1 for Model A; p, r, β, ω and T_1 (in that order for Models B through E.
BI(I)	Vector of coefficient names.
EXF(A,B)	Function to calculate exp(A) erfc(B).
INDEX (I)	Index for each coefficient. If INDEX(I) = 0, the coefficient B(I) is known and kept constant in the program. If INDEX(I) = 1, the coefficient is assumed to be unknown and fitted to the data. At least two coefficient need to be unknown.
MIT	Maximum number of iterations allowed in the least-squares analysis.
MODE	Model number specifying the type of transport model and boundary conditions to be used (see text).
NC	Number of cases considered.
NDATA	Data input code. If NDATA = 1, new data are read in for that particular case. If NDATA = 0, the data of the previous case (or part of them) are used for the new problem. This code allows one to fit the same data to different models.
NIT	Iteration number during least-squares analysis.
NOB	Number of observations (cannot exceed 90 with presently dimensioned arrays).
SSQ, SUMB	Residual sum of squares.
STOPCR	Stop criterion. The iterative curve-fitting process stops when the relative change in the ratio of all coefficients becomes less than STOPCR.
TITLE	Vector containing information of title card (input label).

X(I), Y(I) Observed effluent data: pore volume and concentration, respectively.

Table A-2. Data input instructions. (From USDA Research Report No. 119, Van Genuchten, February, 1981.)

Card	Column	Format	Variable	Comment
1	1- 5	15	NC	Number of cases considered. The remaining cards are read in for each case. If NDATA = 0 on card 2, data cards 7, etc. are not needed for that particular case.
2	1- 5	15	MODE	Model number.
2	6-10	15	NDATA	Data input code.
2	11-15	15	MIT	Maximum number of iterations.
2	16-20	15	NOB	Number of observations.
3	1-80	20A4	TITLE	Information card.
4	1- 6	A4,A2	BI(1)	Coefficient name for P
4	11-16	A4,A2	BI(2)	Coefficient name for R.
4	21-26	A4,A2	BI(3)	Coefficient name for B(3).
4	31-36	A4,A2	BI(4)	Coefficient name for B(4).
4	41-46	A4,A2	BI(4)	Coefficient name for B(5).
5	1-10	F10.0	B(1)	Initial value of P.
5	11-20	F10.0	B(2)	Initial value of R.
5	21-30	F10.0	B(3)	Initial value of B(3).
5	31-40	F10.0	B(4)	Initial value of B(4).
5	41-50	F10.0	B(5)	Initial value of B(5).
6	1- 5	15	INDEX(1)	Index for each coefficient.
6	6- 10	15	INDEX(2)	See text for explanation.
6	11- 15	15	INDEX(3)	
6	16- 20	15	INDEX(4)	
6	21- 25	15	INDEX(5)	
7, etc.	1-10	F10.0	X(I)	Value of observed pore volume.
7, etc.	11-20	F10.0	Y(I)	Value of observed concentration. Card 7 is repeated NOB times.

```
      PROGRAM SHALE (INPUT,OUTPUT,TAPE5=INPUT,TAPE6=OUTPUT)
C
C     ******************************************************************
C     *                                                                *
C     *    NON-LINEAR LEAST-SQUARES ANALYSIS     CFITIM                *
C     *                                                                *
C     *    ---------------- INPUT INFORMATION ----------------          *
C     *                                                                *
C     *    CARD 1: NUMBER OF CASES CONSIDERED: NC (I5)                 *
C     *                                                                *
C     *           THE NEXT CARDS ARE REPEATED NC TIMES                 *
C     *                                                                *
C     *    CARD 2: MODEL  NUMBER (MODE), DATA INPUT CODE (NDATA),      *
C     *            MAXIMUM NUMBER OF ITERATIONS (MIT) AND NUMBER       *
C     *            OF OBSERVATIONS (NOB)  (4I5)                        *
C     *            MODE=1,2: EQUILIBRIUM TRANSPORT (MODEL A)           *
C     *                =3,4: NON-EQUILIBRIUM TRANSPORT (MODEL B)       *
C     *                =5,6: ONE-SITE KINETIC ADSORPTION (MODEL D)     *
C     *                =1,3,5: FIRST-TYPE BOUNDARY CONDITION           *
C     *                =2,4,6: THIRD-TYPE BOUNDARY CONDITION           *
C     *            NDATA=0: SAME DATA AS PREVIOUS CASE                 *
C     *                 =1: NEW DATA                                   *
C     *    CARD 3: INFORMATION CARD  (20A4)                            *
C     *    CARD 4: NAMES OF THE COEFFICIENTS  3(A4,A2,4X)              *
C     *    CARD 5: INITIAL ESTIMATES OF COEFFICIENTS (3F10.0)          *
C     *    CARD 6: INDEX FOR EACH COEFFICIENT  5(I5)                   *
C     *            =0  IF COEFFICIENT IS KNOWN (CONSTANT)              *
C     *            =1  IF COEFFICIENT IS UNKNOWN                       *
C     *                                                                *
C     *            THE NEXT CARDS ARE READ IN ONLY IF NDATA=1          *
C     *                                                                *
C     *    CARD 7,ETC.: EXPERIMENTAL DATA: PORE VOLUME AND             *
C     *           CONCENTRATION (NOB CARDS)  (2F10.0)                  *
C     *                                                                *
C     ******************************************************************
C
C
      DIMENSION Y(90),X(90),F(90),R(90),DELZ(90,5),B(10),E(5),TH(10),
     1P(5),PHI(5),Q(5),LSORT(90),TB(10),A(5,5),BI(10),TITLE(20),D(5,5),
     2INDEX(5)
      DATA STOPCR/0.0005/
C
C     ----- READ NUMBER OF CASES -----
      READ(5,1006) NC
      DO 120 NCASE=1,NC
      WRITE(6,1000)
C
C     ----- READ INPUT PARAMETERS -----
      READ(5,1006) MODE,NDATA,MIT,NOB
```

```
      M=(MODE-1)/2
      IF(M.EQ.0) WRITE(6,1021)
      IF(M.EQ.1) WRITE(6,1022)
      IF(M.EQ.2) WRITE(6,1023)
      N=MODE-2*M
      IF(N.EQ.1) WRITE(6,1024)
      IF(N.EQ.2) WRITE(6,1025)
      NU=3
      IF(MODE.GT.2) NU=5
      NU1=NU+1
      NU2=2*NU
      READ(5,1001) TITLE
      WRITE(6,1002) TITLE
C
C     ----- READ COEFFICIENTS NAMES -----
      READ(5,1004) (BI(I),I=1,NU2)
C
C     ----- READ INITIAL ESTIMATES -----
      READ(5,1005) (B(I),I=NU1,NU2)
      IF(M.EQ.2) B(8)=1./B(7)
C
C     ----- READ INDICES -----
      READ(5,1006) (INDEX(I),I=1,NU)
      IF(M.EQ.2) INDEX(3)=0
      WRITE(6,1007)
      DO 4  I=1,NU
      J=2*I-1
    4 WRITE(6,1008) I,BI(J),BI(J+1),B(I+NU)
      IF(NDATA.EQ.0) GO TO 10
C
C     ----- READ AND WRITE EXPERIMENTAL DATA -----
      DO 6 I=1,NOB
    6 READ(5,1005) X(I),Y(I)
   10 WRITE(6,1009)
      DO 12 I=1,NOB
   12 WRITE(6,1010) I,X(I),Y(I)
C
C     ----------
      NP=0
      DO 14 I=NU1,NU2
      TB(I)=B(I)
      IF(INDEX(I-NU).EQ.0) GO TO 14
      NP=NP+1
      K=2*NP-1
      J=2*(I-NU)-1
      BI(K)=BI(J)
      BI(K+1)=BI(J+1)
      B(NP)=B(I)
      TB(NP)=B(I)
      TH(NP)=B(NP)
   14 TH(I)=B(I)
C
C     ----------
      GA=0.02
```

```
      NIT=0
      NP2=2*NP
      CALL MODEL(TH,F,NOB,X,INDEX,MODE)
      SSQ=0.
      DO 32 I=1,NOB
      R(I)=Y(I)-F(I)
   32 SSQ=SSQ+R(I)*R(I)
      WRITE(6,1011) (BI(J),BI(J+1),J=1,NP2,2)
      WRITE(6,1012) NIT,SSQ,(B(I),I=1,NP)
C
C     ----- BEGIN OF ITERATION -----
   34 NIT=NIT+1
      GA=0.1*GA
      DO 38 J=1,NP
      TEMP=TH(J)
      TH(J)=1.01*TH(J)
      Q(J)=0
      CALL MODEL(TH,DELZ(1,J),NOB,X,INDEX,MODE)
      DO 36 I=1,NOB
      DELZ(I,J)=DELZ(I,J)-F(I)
   36 Q(J)=Q(J)+DELZ(I,J)*R(I)
      Q(J)=100.*Q(J)/TH(J)
C
C     ----- Q=XT*R (STEEPEST DESCENT) -----
   38 TH(J)=TEMP
      DO 44 I=1,NP
      DO 42 J=1,I
      SUM=0
      DO 40 K=1,NOB
   40 SUM=SUM+DELZ(K,I)*DELZ(K,J)
      D(I,J)=10000.*SUM/(TH(I)*TH(J))
   42 D(J,I)=D(I,J)
   44 E(I)=SQRT(D(I,I))
   50 DO 52 I=1,NP
      DO 52 J=1,NP
   52 A(I,J)=D(I,J)/(E(I)*E(J))
C
C     ----- A IS THE SCALED MOMENT MATRIX -----
      DO 54 I=1,NP
      P(I)=Q(I)/E(I)
      PHI(I)=P(I)
   54 A(I,I)=A(I,I)+GA
      CALL MATINV(A,NP,P)
C
C     ----- P/E IS THE CORRECTION VECTOR -----
      STEP=1.0
   56 DO 58 I=1,NP
   58 TB(I)=P(I)*STEP/E(I)+TH(I)
      DO 62 I=1,NP
      IF(TH(I)*TB(I))66,66,62
   62 CONTINUE
      SUMB=0
      CALL MODEL(TB,F,NOB,X,INDEX,MODE)
      DO 64 I=1,NOB
```

```
      R(I)=Y(I)-F(I)
   64 SUMB=SUMB+R(I)*R(I)
   66 SUM1=0.0
      SUM2=0.0
      SUM3=0.0
      DO 68 I=1,NP
      SUM1=SUM1+P(I)*PHI(I)
      SUM2=SUM2+P(I)*P(I)
   68 SUM3=SUM3+PHI(I)*PHI(I)
      ANGLE=57.2958*ACOS(SUM1/SQRT(SUM2*SUM3))
C
C     ----------
      DO 72 I=1,NP
      IF(TH(I)*TB(I))74,74,72
   72 CONTINUE
      IF((SUMB-SSQ).LT.1.D-08)GO TO 80
   74 IF(ANGLE-30.0)76,76,78
   76 STEP=0.5*STEP
      GO TO 56
   78 GA=10.*GA
      GO TO 50
C
C     ----- PRINT COEFFICIENTS AFTER EACH ITERATION -----
   80 CONTINUE
      DO 82 I=1,NP
   82 TH(I)=TB(I)
      WRITE(6,1012) NIT,SUMB,(TH(I),I=1,NP)
      DO 86 I=1,NP
      IF(ABS(P(I)*STEP/E(I))/(1.0E-20+ABS(TH(I)))-STOPCR) 86,86,94
   86 CONTINUE
      GO TO 96
   94 SSQ=SUMB
      IF(NIT.LE.MIT) GO TO 34
C
C     ----- END OF ITERATION LOOP -----
   96 CONTINUE
      CALL MATINV(D,NP,P)
C
C     ----- WRITE CORRELATION MATRIX -----
      DO 98 I=1,NP
   98 E(I)=SQRT(AMAX1(D(I,I),1.E-20))
      WRITE(6,1013) (I,I=1,NP)
      DO 102 I=1,NP
      DO 100 J=1,I
  100 A(J,I)=D(J,I)/(E(I)*E(J))
  102 WRITE(6,1014) I,(A(J,I),J=1,I)
C
C     ----- CALCULATE 95% CONFIDENCE INTERVAL -----
      Z=1./FLOAT(NOB-NP)
      SDEV=SQRT(Z*SUMB)
      TVAR=1.96+Z*(2.3779+Z*(2.7135+Z*(3.187936+2.466666*Z**2)))
      WRITE(6,1015)
      DO 108 I=1,NP
      SECOEF=E(I)*SDEV
```

```
      TVALUE=TH(I)/SECOEF
      TSEC=TVAR*SECOEF
      TMCOE=TH(I)-TSEC
      TPCOE=TH(I)+TSEC
      J=2*I-1
  108 WRITE(6,1016) I,BI(J),BI(J+1),TH(I),SECOEF,TVALUE,TMCOE,TPCOE
C
C     ----- PREPARE FINAL OUTPUT -----
      LSORT(1)=1
      DO 116 J=2,NOB
      TEMP=R(J)
      K=J-1
      DO 111 L=1,K
      LL=LSORT(L)
      IF(TEMP-R(LL)) 112,112,111
  111 CONTINUE
      LSORT(J)=J
      GO TO 116
  112 KK=J
  113 KK=KK-1
      LSORT(KK+1)=LSORT(KK)
      IF(KK-L) 115,115,113
  115 LSORT(L)=J
  116 CONTINUE
      WRITE(6,1017)
      DO 118 I=1,NOB
      J=LSORT(NOB+1-I)
  118 WRITE(6,1018) I,X(I),Y(I),F(I),R(I),J,X(J),Y(J),F(J),R(J)
      WRITE(6,1020)
  120 CONTINUE
C
C     ----- END OF PROBLEM -----
 1000 FORMAT(1H1,10X,82(1H*)/11X,1H*,80X,1H*/11X,1H*,10X,'NON-LINEAR LEA
     1ST SQUARES ANALYSIS',37X,1H*/11X,1H*,80X,1H*)
 1001 FORMAT(20A4)
 1002 FORMAT(11X,1H*,20A4,1H*/11X,1H*,80X,1H*/11X,82(1H*))
 1004 FORMAT(5(A4,A2,4X))
 1005 FORMAT(5F10.0)
 1006 FORMAT(5I5)
 1007 FORMAT(//11X,'INITIAL VALUES OF COEFFICIENTS'/11X,30(1H=)/12X,'NO'
     1,6X,'NAME',9X,'INITIAL VALUE')
 1008 FORMAT(11X,I3,5X,A4,A2,4X,F12.3)
 1009 FORMAT(//11X,'OBSERVED DATA',/11X,13(1H=)/11X,'OBS. NO.',5X,'PORE
     1VOLUME',5X,'CONCENTRATION')
 1010 FORMAT(11X,I5,5X,F12.4,4X,F12.4)
 1011 FORMAT(//11X,'ITERATION',6X,'SSQ',4X,5(7X,A4,A2))
 1012 FORMAT(11X,I5,5X,F11.7,2X,5F13.5)
 1013 FORMAT(1H1,10X,'CORRELATION MATRIX'/11X,18(1H=)/14X,10(4X,I2,5X))
 1014 FORMAT(11X,I3,10(2X,F7.4,2X))
 1015 FORMAT(///,11X,'NON-LINEAR LEAST SQUARES ANALYSIS, FINAL RESULTS'
     1/11X,48(1H=)//72X,'95% CONFIDENCE LIMITS'/11X,'VARIABLE',4X,'NAME'
     2,8X,'VALUE',8X,'S.E.COEFF.',3X,'T-VALUE',5X,'LOWER',10X,'UPPER')
 1016 FORMAT(14X,I2,6X,A4,A2,2X,F12.5,5X,F9.4,4X,F8.2,2X,F9.4,6X,F9.4)
 1017 FORMAT(//10X,9(1H-),'ORDERED BY COMPUTER INPUT',10(1H-), 7X,12(1H-
```

```
     1),'ORDERED BY RESIDUALS',12(1H-)/18X,'PORE',6X,'CONCENTRATION',
     26X,'RESI-',18X,'PORE',6X,'CONCENTRATION',6X,'RESI-'/10X,'NO',4X,
     3'VOLUME',6X,'OBS.',4X,'FITTED',6X,'DUAL',10X,'NO',4X,'VOLUME',6X,
     4'OBS.',4X,'FITTED',6X,'DUAL')
 1018 FORMAT(10X,I2,4F10.3,10X,I2,4F10.3)
 1020 FORMAT(///11X,'END OF PROBLEM'/11X,14(1H=))
 1021 FORMAT(11X,1H*,10X,'EQUILIBRIUM TRANSPORT (MODEL A)',39X,1H*)
 1022 FORMAT(11X,1H*,10X,'NON-EQUILIBRIUM TRANSPORT (MODEL B)',35X,1H*)
 1023 FORMAT(11X,1H*,10X,'ONE-SITE KINETIC ADSORPTION (MODEL D)',33X,1H*
     1)
 1024 FORMAT(11X,1H*,10X,'FIRST-TYPE BOUNDARY CONDITION',41X,1H*)
 1025 FORMAT(11X,1H*,10X,'THIRD-TYPE BOUNDARY CONDITION',41X,1H*)
      STOP
      END
      SUBROUTINE MODEL(B,Y,NOB,X,INDEX,MODE)
C
C     PURPOSE: TO CALCULATE CONCENTRATIONS FOR GIVEN PORE VOLUME
C
      DIMENSION B(10),Y(90),X(90),INDEX(5),XG(20),W(20)
      DATA XG/.03877242,.1160841,.1926976,.2681522,.3419941,.4137792,
     1.4830758,.5494671,.6125539,.6719567,.7273183,.7783057,.8246122,
     2.8659595,.9020988,.9328128,.9579168,.9772599,.9907262,.9982377/
      DATA W/.07750595,.07703982,.07611037,.07472317,.07288658,.07061165
     1,.06791204,.06480401,.06130624,.05743977,.05322785,.04869581,.0438
     27091,.03878217,.03346019,.02793701,.02224585,.01642106,.01049828,.
     300452128/
C
C     ---------------
      K=0
      IF(MODE.LE.2) GO TO 12
C
C     ----- SOLUTION FOR NON-EQUILIBRIUM TRANSPORT (MODEL B) -----
      DO 2 I=6,10
      IF(INDEX(I-5).EQ.0) GO TO 2
      K=K+1
      B(I)=B(K)
    2 CONTINUE
      P=B(6)
      R=B(7)
      IF(MODE.GE.5) B(8)=1./R
      BETA=AMIN1(B(8),.9999E00)
      OMEGA=B(9)
      DO 10 J=1,NOB
      DO 8 M=1,2
      C=0.0
      T=X(J)+(1-M)*B(10)
      IF(T.LE.0.) GO TO 6
      A=SQRT(1.+.05*P)
      T2=AMIN1(T,BETA*R*(1.+40.*(1.+A)/P))
      T1=AMAX1(0.E00,BETA*R*(1.+40.*(1.-A)/P))
      IF(T2.LE.T1) GO TO 6
      DO 4 I=1,20
      TAU=0.5*(T1+T2+(T2-T1)*XG(I))
      C=C+W(I)*CCO(P,R,BETA,OMEGA,T,TAU,MODE)
```

```
      TAU=0.5*(T1+T2+(T1-T2)*XG(I))
    4 C=C+W(I)*CCO(P,R,BETA,OMEGA,T,TAU,MODE)
      C=0.5*(T2-T1)*C
    6 IF(M.EQ.2) GO TO 8
      Y(J)=C
    8 CONTINUE
   10 Y(J)=Y(J)-C
      RETURN
C
C     ----- SOLUTION FOR EQUILIBRIUM TRANSPORT (MODEL A) -----
   12 DO 14 I=4,6
      IF(INDEX(I-3).EQ.0) GO TO 14
      K=K+1
      B(I)=B(K)
   14 CONTINUE
      E=0.0
      P=B(4)
      R=B(5)
      DO 18 J=1,NOB
      DO 16 M=1,2
      C=0.0
      T=X(J)+(1-M)*B(6)
      IF(T.LE.0.) GO TO 18
      CM=0.5*(R-T)*SQRT(P/(R*T))
      CP=0.5*(R+T)*SQRT(P/(R*T))
      C=0.5*EXF(E,CM)+0.5*EXF(P,CP)
      IF(MODE.EQ.2) C=C+SQRT(.3183099*P*T/R)*EXF(-CM*CM,E)-0.5*(2.+P+P*
     1T/R)*EXF(P,CP)
      IF(M.EQ.2) GO TO 18
      Y(J)=C
   16 CONTINUE
   18 Y(J)=Y(J)-C
      RETURN
      END
      FUNCTION CCO(P,R,BETA,OMEGA,T,TAU,MODE)
C
C     PURPOSE: TO CALCULATE THE ARGUMENT UNDER THE INTEGRAL SIGN
C
      CCO=0.0
      BER=BETA*R
      CM=P*(BER-TAU)**2/(4.*BER*TAU)
      C=.2820948*SQRT(P*BER/TAU**3)*EXP(-CM)
      IF((MODE.EQ.3).OR.(MODE.EQ.5)) GO TO 2
      CP=(BER+TAU)*SQRT(P/(4.*BER*TAU))
      C=2.*C*TAU/BER-0.5*P*EXF(P,CP)/BER
    2 IF(C.LT.1.D-07) RETURN
      EPSI=OMEGA*TAU/BER
      ETHA=OMEGA*(T-TAU)/(R-BER)
      CCO=C*GOLD(EPSI,ETHA)
      RETURN
      END
      FUNCTION GOLD(X,Y)
C
C     PURPOSE: TO CALCULATE J(X,Y)
```

```
C
      GOLD=0.0
      BF=0.0
      E=2.*SQRT(X*Y)
      Z=X+Y-E
      IF(Z.GT.17.) GO TO 8
      IF(E.NE.0.) GO TO 2
      GOLD=EXP(-X)
      RETURN
    2 A=AMAX1(X,Y)
      B=AMIN1(X,Y)
      NT=11.+2.*B+0.3*A
      IF(NT.GT.25) GO TO 6
      I=0
      IF(X.LT.Y) I=1
      GXY=1.+I*(B-1.)
      GX=1.0
      GY=GXY
      GZ=1.0
      DO 4 K=1,NT
      GX=GX*A/K
      GY=GY*B/(K+I)
      GZ=GZ+GX
    4 GXY=GXY+GY*GZ
      GOLD=GXY*EXP(-X-Y)
      GO TO 8
    6 DA=SQRT(A)
      DB=SQRT(B)
      P=3.75/E
      B0=(.3989423+P*(.01328592+P*(.00225319-P*(.00157565-P*(.00916281-P
     1*(.02057706-P*(.02635537-P*(.01647633-.00392377*P)))))))/SQRT(E)
      BF=B0*EXP(-Z)
      P=1./(1.+.3275911*(DA-DB))
      ERF=P*(.2548296-P*(.2844967-P*(1.421414-P*(1.453152-P*1.061405))))
      P=0.25/E
      C0=1.-1.772454*(DA-DB)*ERF
      C1=0.5-Z*C0
      C2=0.75-Z*C1
      C3=1.875-Z*C2
      C4=6.5625-Z*C3
      SUM=.1994711*(A-B)*P*(C0+1.5*P*(C1+1.666667*P*(C2+1.75*P*(C3+P*(C4
     1*(1.8-3.3*P*Z)+97.45313*P)))))
      GOLD=0.5*BF+(.3535534*(DA+DB)*ERF+SUM)*BF/(B0*SQRT(E))
    8 IF(X.LT.Y) GOLD=1.+BF-GOLD
      RETURN
      END
      FUNCTION EXF(A,B)
C
C     PURPOSE: TO CALCULATE EXP(A) ERFC(B)
C
      EXF=0.0
      IF((ABS(A).GT.170).AND.(B.LE.0.)) RETURN
      IF(B.NE.0.0) GO TO 1
      EXF=EXP(A)
```

```
      RETURN
    1 C=A-B*B
      IF((ABS(C).GT.170).AND.(B.GT.0.)) RETURN
      IF(C.LT.-170.) GO TO 4
      X=ABS(B)
      IF(X.GT.3.0) GO TO 2
      T=1./(1.+.3275911*X)
      Y=T*(.2548296-T*(.2844967-T*(1.421414-T*(1.453152-1.061405*T))))
      GO TO 3
    2 Y=.5641896/(X+.5/(X+1./(X+1.5/(X+2./(X+2.5/(X+1.))))))
    3 EXF=Y*EXP(C)
    4 IF(B.LT.0.0) EXF=2.*EXP(A)-EXF
      RETURN
      END
      SUBROUTINE MATINV(A,NP,B)
      DIMENSION A(5,5),B(10),INDEX(5,2)
      DO 2 J=1,5
    2 INDEX(J,1)=0
      I=0
    4 AMAX=-1.0
      DO 11 J=1,NP
      IF(INDEX(J,1)) 11,6,11
    6 DO 10 K=1,NP
      IF(INDEX(K,1)) 10,8,10
    8 P=ABS(A(J,K))
      IF(P.LE.AMAX) GO TO 10
      IR=J
      IC=K
      AMAX=P
   10 CONTINUE
   11 CONTINUE
      IF(AMAX) 30,30,14
   14 INDEX(IC,1)=IR
      IF(IR.EQ.IC) GO TO 18
      DO 16 L=1,NP
      P=A(IR,L)
      A(IR,L)=A(IC,L)
   16 A(IC,L)=P
      P=B(IR)
      B(IR)=B(IC)
      B(IC)=P
      I=I+1
      INDEX(I,2)=IC
   18 P=1./A(IC,IC)
      A(IC,IC)=1.0
      DO 20 L=1,NP
   20 A(IC,L)=A(IC,L)*P
      B(IC)=B(IC)*P
      DO 24 K=1,NP
      IF(K.EQ.IC) GO TO 24
      P=A(K,IC)
      A(K,IC)=0.0
      DO 22 L=1,NP
   22 A(K,L)=A(K,L)-A(IC,L)*P
```

```
      B(K)=B(K)-B(IC)*P
   24 CONTINUE
      GO TO 4
   26 IC=INDEX(I,2)
      IR=INDEX(IC,1)
      DO 28 K=1,NP
      P=A(K,IR)
      A(K,IR)=A(K,IC)
   28 A(K,IC)=P
      I=I-1
   30 IF(I) 26,32,26
   32 RETURN
      END
```

APPENDIX B. Leaching column Text Data

Table B-1. Media A: 0.420-1.190mm Grain Size Paraho Spent Shale

Elapsed Time (Hours)	Temperature Corrected Electrical Conductivity (umhos/cm) Test #1 (Q=130.47 ml/hr)	Test #2 (Q=131.69 ml/hr)	Test #3 (Q=164.4 ml/hr)
0			
0.5	8171	8980	8824
1.0	8441	9109	9020
1.5	8409	9043	9101
2.0	8485	9022	9112
2.5	8501	9037	9056
3.0	8549	9054	9007
3.5	8587	9048	8975
4.0	8592	9052	8986
4.5	8571	9084	8947
5.0	8603	9106	8947
5.5	8608	9131	8980
6.0	8613	9178	8985
6.5	8661	9249	9028
7.0	8694	9302	9038
7.5	8747	9377	8985
8.0	8785	9459	----
8.5	8806	9544	8710
9.0	8860	9619	----
9.5	8908	9712	----
10.0	----	----	----
10.5	8795	9833	----
11.0	8758	9895	----
11.5	8678	9908	----
12.0	8630	9937	----
12.5	8576	9937	6897
13.0	8490	9905	6434
13.5	8409	9881	6337
14.0	8345	9806	----
14.5	8231	9716	6000
15.0	8087	9580	----
15.5	7962	9458	5816
16.0	7833	9307	5652
16.5	7718	9152	5912
17.0	7589	8969	5642
17.5	7460	8775	5642
18.0	7333	8586	5652
18.5	7190	8376	5112
19.0	7050	8171	5102
19.5	6923	7992	----
20.0	6804	7787	4571
20.5	6685	7592	4815
21.0	6568	7412	4763
21.5	6461	7241	4729
22.0	6330	7044	4693

Table B-1 (continued)

Elapsed Time (Hours)	Temperature Corrected Electrical Conductivity (μmhos/cm) Test #1 (Q=130.47 ml/hr)	Test #2 (Q=131.69 ml/hr)	Test #3 (Q=164.4 ml/hr)
22.5	6233	6905	----
23.0	6102	6752	4601
23.5	6016	6633	4733
24.0	5951	6500	4662
24.5	5875	6242	4607
25.0	5843	6241	4554
25.5	5746	6165	4539
26.0	5660	6078	4505
26.5	5639	5842	4457
27.0	5543	5890	4406
27.5	5478	5864	4320
28.0	5457	5810	4291
28.5	5381	5767	4264
29.0	5339	5714	4213
29.5	5327	5671	4138
30.0	5274	5617	4116
30.5	5230	5574	4087
31.0	5187	5520	3998
31.5	5154	5488	3970
32.0	5111	5434	3952
32.5	5077	5401	3916
33.0	5023	5347	3852
33.5	4991	5304	3809
34.0	4905	5261	3777
34.5	4883	5228	3734
35.0	4840	5185	3741
35.5	4849	5162	3677
36.0	4806	5108	3645
36.5	4774	5065	3645
37.0	4730	5022	3599
37.5	4707	4999	3595
38.0	4683	4965	3556
38.5	4650	4921	3531
39.0	4618	4889	3473
39.5	4588	4847	3473
40.0	4555	4804	3465
40.5	4531	4780	3437
41.0	4499	4748	3411
41.5	4469	4696	3385
42.0	4436	4674	3363
42.5	4412	4640	3337
43.0	4371	4599	3289
43.5	4350	4566	3268
44.0	4325	4553	3235
44.5	4285	4512	3268
45.0	4271	4488	3241
45.5	4231	4447	3176
46.0	4209	4415	3160

Table B-1 (continued)

Elapsed Time (Hours)	Temperature Corrected Electrical Conductivity (umhos/cm) Test #1 (Q=130.47 ml/hr)	Test #2 (Q=131.69 ml/hr)	Test #3 (Q=164.4 ml/hr)
46.5	4195	4390	3133
47.0	4163	4369	3111
47.5	4133	4328	3139
48.0	4065	4314	3127
48.5	4043	4293	3084
49.0	4065	4260	3084
49.5	4000	4238	3030
50.0	3978	4217	3013
50.5	4000	4195	3018
51.0	3928	4155	3013
51.5	3899	4126	2986
52.0	3895	4112	2970
52.5	3906	4090	2948
53.0	3874	4058	2932
53.5	3852	4036	2884
54.0	3830	4014	2873
54.5	3809	3982	2857
55.0	3794	3967	2852
55.5	3765	3938	2830
56.0	3744	3917	2814
56.5	3729	3902	2809
57.0	3700	3863	2798
57.5	3679	3841	2782
58.0	3657	3819	2755
58.5	3607	3791	2755
59.0	3614	3787	2744
59.5	3592	3765	2727
60.0	3581	3733	2717
60.5	3566	3729	2706
61.0	3545	3696	2701
61.5	3523	3675	2684
62.0	3508	3660	2673
62.5	3490	3631	2662
63.0	3475	3616	2651
63.5	3443	3595	2629
64.0	3438	3580	2634
64.5	3410	3562	2612
65.0	3399	3540	2602
65.5	3377	3519	2580
66.0	3356	3497	2583
66.5	3351	3482	2572
67.0	3329	3460	2562
67.5	3314	3444	2540
68.0	3259	3423	2529
68.5	3243	3418	2523
69.0	3265	3396	2516
69.5	3237	3368	2538
70.0	3220	3351	2494

Table B-1 (continued)

Elapsed Time (Hours)	Temperature Corrected Electrical Conductivity (umhos/cm) Test #1 (Q=130.47 ml/hr)	Test #2 (Q=131.69 ml/hr)	Test #3 (Q=164.4 ml/hr)
70.5	3188	3330	2479
71.0	-----	3306	2468
71.5	----	3295	----
72.0	3127	3278	----

Table B-2. Media B: 1.190-2.000mm Grain Size Paraho Spent Shale

Elapsed Time (Hours)	Temperature Corrected Electrical Conductivity (μmhos/cm) Test #1 (Q=121.94 ml/hr)	Test #2* (Q=116.75 ml/hr)	Test #3 (Q=152.74 ml/hr)
0	----	----	----
0.5	----	9420	7583
1.0	8530	9440	7888
1.5	8595	9430	7993
2.0	8644	9410	8091
2.5	8671	9430	8124
3.0	8682	----	8165
3.5	8715	9460	8197
4.0	8715	9470	8230
4.5	8660	9450	8247
5.0	8666	9510	8279
5.5	8688	9530	8301
6.0	8699	9500	8285
6.5	8731	9330	8307
7.0	8460	8950	8231
7.5	7884	8750	8081
8.0	7431	8490	----
8.5	7083	8310	7443
9.0	6777	8160	----
9.5	6453	8020	----
10.0	6115	7930	----
10.5	5799	7810	----
11.0	5536	7750	----
11.5	5384	7640	----
12.0	5199	7540	----
12.5	5067	7380	5547
13.0	4916	7340	4788
13.5	4805	7240	4618
14.0	4685	7160	----
14.5	4608	7050	4570
15.0	4526	6990	----
15.5	4439	6870	4484
16.0	4348	6800	4313
16.5	4268	6770	4553
17.0	4202	6670	4561
17.5	4133	6600	4467
18.0	4085	6530	4438
18.5	4030	6460	----
19.0	3963	6380	----
19.5	3919	6350	----
20.0	3882	6260	4272
20.5	3838	6180	4131
21.0	3794	6150	4124
21.5	----	6080	3777
22.0	----	5990	3802
22.5	3676	5940	----
23.0	----	5910	3734
23.5	----	5800	3752

Table B-2 (continued)

Elapsed Time (Hours)	Temperature Corrected Electrical Conductivity (μmhos/cm) Test #1 (Q=121.94 ml/hr)	Test #2* (Q=116.75 ml/hr)	Test #3 (Q=152.74 ml/hr)
24.0	----	----	3696
24.5	3506	----	3671
25.0	3460	----	3607
25.5	3438	5640	3556
26.0	3399	5590	3510
26.5	3371	5550	3469
27.0	3365	5510	3420
27.5	3326	5470	3398
28.0	3298	5430	3371
28.5	3237	5380	3329
29.0	3242	5360	3312
29.5	3215	5310	3291
30.0	3111	5280	3270
30.5	3187	5240	3242
31.0	3165	5210	3198
31.5	3178	5160	3178
32.0	3181	5130	3140
32.5	3127	5100	3103
33.0	3105	5060	3060
33.5	3089	5040	3028
34.0	----	5010	2985
34.5	----	4970	2953
35.0	----	4920	2927
35.5	----	4900	2905
36.0	----	4870	2884
36.5	2954	4850	2862
37.0	2959	4790	2852
37.5	2943	4770	2836
38.0	----	4750	2809
38.5	----	4720	2793
39.0	----	4690	2798
39.5	----	4660	2766
40.0	----	4620	2755
40.5	----	4590	2728
41.0	----	4560	2722
41.5	----	4520	2706
42.0	----	4480	2695
42.5	----	4450	2678
43.0	----	4430	2673
43.5	----	4400	2662
44.0	----	4380	2640
44.5	----	4350	2629
45.0	----	4330	2623
45.5	----	4300	2612
46.0	----	4280	2606
46.5	----	4250	2591
47.0	----	4220	2580
47.5	----	4190	2574

Table B-2 (continued)

Elapsed Time (Hours)	Temperature Corrected Electrical Conductivity (umhos/cm) Test #1 (Q=121.94 ml/hr)	Test #2* (Q=116.75 ml/hr)	Test #3 (Q=152.74 ml/hr)
48.0	2662	4180	2554
48.5	2613	4140	2554
49.0	2587	4100	2543
49.5	2591	4080	2543
50.0	2547	4080	2527
50.5	2510	4060	2512
51.0	2472	4030	2516
51.5	2462	4010	2501
52.0	2440	3990	2486
52.5	2446	3970	2486
53.0	2431	3950	2470
53.5	2409	3920	2455
54.0	2394	3900	2455
54.5	2383	3870	2440
55.0	2367	3850	2433
55.5	2367	3830	2433
56.0	2346	3820	2408
56.5	2396	3790	2401
57.0	2374	3770	2367
57.5	2352	3760	2384
58.0	2357	3730	2337
58.5	2324	3710	2378
59.0	2328	3700	2324
59.5	2307	3680	2339
60.0	2285	3660	2361
60.5	2285	3630	2350
61.0	2274	3600	2324
61.5	2278	3580	2328
62.0	2267	----	2296
62.5	2245	3560	2283
63.0	2235	3540	2305
63.5	2245	3520	2305
64.0	2239	3500	2255
64.5	2228	3480	2255
65.0	2217	3470	2255
65.5	2206	3450	2266
66.0	2199	3430	2267
66.5	2203	3420	2235
67.0	2181	3400	2224
67.5	2174	3390	2224
68.0	2159	3370	2202
68.5	2148	3360	2228
69.0	2152	3350	2221
69.5	2137	3330	2221
70.0	2119	3320	2177
70.5	2104	3300	2162
71.0	2104	3290	2195

Table B-2 (continued)

Elapsed Time (Hours)	Temperature Corrected Electrical Conductivity (μmhos/cm) Test #1 (Q=121.94 ml/hr)	Test #2* (Q=116.75 ml/hr)	Test #3 (Q=152.74 ml/hr)
71.5	2093	3270	----
72.0	----	3270	2147

* EC values given for Test B-2 are not corrected for temperature.

Table B-3. Media C: 2.362-3.327mm Grain Size Paraho Spent Shale

Elapsed Time (Hours)	Temperature Corrected Electrical Conductivity (umhos/cm) Test #1* (Q=116.75 ml/hr)	Test #2 (Q=125.61 ml/hr)	Test #3 (Q=163.67 ml/hr)
0	----	----	----
0.5	3490	----	7638
1.0	6970	8127	8182
1.5	8120	8138	8319
2.0	8470	8186	8351
2.5	8680	8204	8375
3.0	----	8258	8402
3.5	8840	8214	8435
4.0	8330	7572	8500
4.5	7750	6593	8484
5.0	7250	6201	8020
5.5	6870	5951	6770
6.0	6920	5788	6122
6.5	6800	5658	5714
7.0	6630	5549	5466
7.5	6530	5452	5262
8.0	6450	5386	----
8.5	6350	5309	4812
9.0	6240	5224	----
9.5	6150	5167	----
10.0	6060	5101	----
10.5	5990	5025	----
11.0	5890	4989	----
11.5	5820	----	----
12.0	5760	4894	----
12.5	5670	4827	4154
13.0	5590	4752	4110
13.5	5530	4696	4049
14.0	5490	4619	----
14.5	5410	4532	4135
15.0	5350	4461	----
15.5	5260	4384	3970
16.0	5220	4304	3891
16.5	5160	4224	4263
17.0	5110	4147	3971
17.5	5040	4077	4139
18.0	4970	4008	4131
18.5	4920	3941	3512
19.0	4860	3875	3618
19.5	4790	3809	----
20.0	4750	3760	3428
20.5	4690	3705	3456
21.0	4630	3650	3428
21.5	4570	----	3413
22.0	4520	----	3405
22.5	4470	3478	----
23.0	4440	----	3285
23.5	4360	----	3273

Table B-3 (continued)

Elapsed Time (Hours)	Temperature Corrected Electrical Conductivity (μmhos/cm) Test #1* (Q=116.75 ml/hr)	Test #2 (Q=125.61 ml/hr)	Test #3 (Q=163.67 ml/hr)
24.0	----	----	3218
24.5	----	3318	3213
25.0	----	3284	3171
25.5	4200	3262	3151
26.0	4210	3223	3124
26.5	4180	3184	3104
27.0	4170	3135	3087
27.5	4130	3085	3055
28.0	4060	3036	3017
28.5	4080	2932	2996
29.0	4010	2894	2959
29.5	4020	2845	2927
30.0	3990	2851	2905
30.5	3970	2786	2857
31.0	3940	2743	2846
31.5	3900	2694	2836
32.0	3880	2673	2809
32.5	3840	2640	2803
33.0	3800	2586	2782
33.5	3770	2580	2771
34.0	3740	----	2750
34.5	3710	----	2739
35.0	3680	----	2723
35.5	3650	----	2701
36.0	3620	----	2691
36.5	3580	2422	2669
37.0	3570	2426	2649
37.5	3540	2409	2643
38.0	3450	----	2617
38.5	3450	----	2600
39.0	3440	----	2584
39.5	3390	----	2562
40.0	3380	----	2550
40.5	3360	----	2535
41.0	3300	----	2529
41.5	3280	----	2523
42.0	3250	----	2501
42.5	3230	----	2484
43.0	3220	----	2478
43.5	3190	----	2467
44.0	3160	----	2445
44.5	3140	----	2435
45.0	3140	----	2428
45.5	3110	----	2417
46.0	3060	----	2400
46.5	3050	----	2385
47.0	3030	----	2374
47.5	3000	2079	2367

Table B-3 (continued)

Elapsed Time (Hours)	Temperature Corrected Electrical Conductivity (μmhos/cm) Test #1* (Q=116.75 ml/hr)	Test #2 (Q=125.61 ml/hr)	Test #3 (Q=163.67 ml/hr)
48.0	2990	2057	2337
48.5	3010	2042	2348
49.0	2990	2039	2326
49.5	2970	2009	2315
50.0	2910	2020	2311
50.5	2900	1984	2296
51.0	2920	1969	2279
51.5	2900	1958	2264
52.0	2880	1947	2257
52.5	2870	1933	2238
53.0	2860	1918	2223
53.5	2850	1918	2208
54.0	2830	1904	2198
54.5	2780	1893	2183
55.0	2780	1879	2176
55.5	2760	1901	2165
56.0	2740	1868	2151
56.5	2730	1886	2155
57.0	2710	1864	2152
57.5	2730	1854	2137
58.0	2690	1846	2123
58.5	2700	1824	2130
59.0	2670	1828	2120
59.5	2630	1806	2081
60.0	2620	1795	2102
60.5	2620	1806	2091
61.0	2590	1795	2077
61.5	2570	1777	2081
62.0	----	1788	2048
62.5	2520	1755	2077
63.0	2520	1744	2056
63.5	2510	1755	2045
64.0	2490	1758	2038
64.5	2500	1736	2005
65.0	2480	1736	1995
65.5	2440	1714	2027
66.0	2450	1718	2038
66.5	2420	1699	1995
67.0	2430	1699	1984
67.5	2420	1702	1973
68.0	2420	1689	1951
68.5	2370	1655	1987
69.0	2390	1658	1969
69.5	2360	1644	1980
70.0	2350	1636	1936
70.5	2340	1622	1933

Table B-3 (continued)

Elapsed Time (Hours)	Temperature Corrected Electrical Conductivity (µmhos/cm) Test #1* (Q=116.75 ml/hr)	Test #2 (Q=125.61 ml/hr)	Test #3 (Q=163.67 ml/hr)
71.0	2330	1622	1955
71.5	2320	1622	----
72.0	2320	----	1897

* EC values given for Test C-1 are not corrected for temperature.

Table B-4. NaCl Leaching Tests: 1.190-20... mm Grain Size Paraho Spent Shale (NaCl solution EC = 7310 μmhos/cm)

Elapsed Time (Hours)	Temperature Corrected Electrical Conductivity (μmhos/cm) NaCl Influent (Q = 131.12 ml/hr)	NaCl Displaced (Q = 131.39 ml/hr)
0	926	7377
0.5	915	7339
1.0	884	7339
1.5	915	7328
2.0	915	7331
2.5	915	7320
3.0	915	7333
3.5	915	7322
4.0	915	7322
4.5	915	7311
5.0	915	7309
5.5	915	7265
6.0	913	6929
6.5	911	6550
7.0	911	6017
7.5	901	5548
8.0	911	5178
8.5	911	4905
9.0	913	4654
9.5	913	4412
10.0	915	4167
10.5	915	3939
11.0	913	3750
11.5	915	3586
12.0	915	3405
12.5	903	3297
13.0	906	3204
13.5	910	3100
14.0	912	3019
14.5	913	2943
15.0	917	2873
15.5	931	2814
16.0	933	2771
16.5	956	2727
17.0	978	2685
17.5	1001	2659
18.0	1056	2654
18.5	1162	2569
19.0	1367	2558
19.5	1707	2522
20.0	2226	2511
20.5	2942	2479
21.0	3749	2500
21.5	4407	2475
22.0	5034	2464
22.5	5417	2453
23.0	5766	2438

Table B-4 (continued)

Elapsed Time (Hours)	Temperature Corrected Electrical Conductivity (umhos/cm) NaCl Influent (Q = 131.12 ml/hr)	NaCl Displaced (Q = 131.39 ml/hr)
23.5	6009	2427
24.0	6261	2406
24.5	6416	2406
25.0	6523	2381
25.5	6602	2370
26.0	6659	2338
26.5	6729	2338
27.0	6789	2313
27.5	6867	2317
28.0	6889	2300
28.5	6922	2294
29.0	6963	2245
29.5	7004	2234
30.0	7042	2217
30.5	7072	2211
31.0	7069	2194
31.5	7065	2172
32.0	7122	2187
32.5	7143	2148
33.0	7153	2131
33.5	7143	2124
34.0	7163	2117
34.5	7189	2102
35.0	7183	2095
35.5	7211	2088
36.0	7226	2070
36.5	7240	2067
37.0	7244	2074
37.5	7289	2070
38.0	7303	2023
38.5	7307	2015
39.0	7331	2022
39.5	7321	1987
40.0	7335	1983
40.5	7350	2004
41.0	7353	1947
41.5	7353	1997
42.0	7357	1954
42.5	7360	1944
43.0	7374	1929
43.5	7378	1929
44.0	7367	1926
44.5	7382	1915
45.0	7385	1901
45.5	7375	1933
46.0	7389	1933
46.5	7385	1890
47.0	7385	1922

Table B-4 (continued)

Elapsed Time (Hours)	Temperature Corrected Electrical Conductivity (umhos/cm) NaCl Influent (Q = 131.12 ml/hr)	NaCl Displaced (Q = 131.39 ml/hr)
47.5	----	1880
48.0	----	1911
48.5	----	1869
49.0	----	1897
49.5	----	1887
50.0	----	1844
50.5	----	1866
51.0	----	1827
51.5	7323	1848
52.0	7334	1837
52.5	7354	1805
53.0	----	1795
53.5	7365	1788
54.0	7375	1812
54.5	7371	1794
55.0	7371	1755
55.5	7385	1780
56.0	7385	1740
56.5	7385	1729
57.0	7385	1722
57.5	7399	1714
58.0	7361	1728
58.5	7379	1742
59.0	7393	1699
59.5	7411	1685
60.0	7401	1717
60.5	7401	1693
61.0	7405	1668
61.5	7409	1672
62.0	7409	1680
62.5	7398	1655
63.0	7412	1610
63.5	7402	1642
64.0	7416	1639
64.5	7416	1593
65.0	7406	1625
65.5	7395	1604
66.0	7385	1579
66.5	7385	1579
67.0	7385	1598
67.5	7403	1576
68.0	7403	1531
68.5	7403	1531
69.0	7403	1566
69.5	7403	1524
70.0	7388	1558

Table B-4 (continued)

Elapsed Time (Hours)	Temperature Corrected Electrical Conductivity (μmhos/cm) NaCl Influent (Q = 131.12 ml/hr)	NaCl Displaced (Q = 131.39 ml/hr)
70.5	7399	1516
71.0	7385	1553
71.5	7371	1511